HYDROGEN EMBRITTLEMENT AND STRESS CORROSION CRACKING OF URANIUM AND URANIUM ALLOYS*

Nicholas J. Magnani
Sandia Laboratories
Albuquerque, New Mexico

INTRODUCTION

The principal reason for interest in uranium is the nuclear behavior of the 235 isotope. However, there has also been interest in depleted† uranium because of its high density ($\rho = 19.1$ g/cm^3) and in some cases its structural properties. Because depleted uranium is a by-product of enriched nuclear fuel, it is less expensive than any other high-density material. Tungsten, with a density of 19.3 g/cm^3, not only has a higher raw material cost but also is more expensive to fabricate. Other elements with densities above 15 g/cm^3, Re, Os, Ir, Pt, Au, and Pu are very expensive. Therefore, in addition to their nuclear applications, uranium and uranium alloys have been used for ballast and counterweights where space is limited such as in aircraft and missiles, for non-nuclear ordnance as an armor penetrator, and for radiation shielding. A uranium radiation shield not only occupies less volume than an equivalent lead shield but can weigh two-thirds as much. Because of their mechanical properties uranium alloys have a great deal of potential as shipping container–shielding for spent reactor fuels where safety requires the containers remain intact in an accident.

One of the problems that have been encountered in the use of uranium and uranium alloys is stress corrosion cracking. In this chapter the effects of environment on the mechanical properties of uranium and uranium alloys will be discussed. The discussion will include both embrittlement and stress corrosion cracking.

* This work was supported by the U.S. Energy Research and Development Administration.

† Depleted uranium is ~99.8% U^{238} and ~0.2% U^{235}, while natural uranium is 99.3% U^{238} and 0.7% U^{235}.

M. G. Fontana et al. (eds.), *Advances in Corrosion Science and Technology*

Polymorphism in Uranium

Uranium exists in three polymorphic forms: an orthorhombic form which is stable below 662°C designated α uranium, a tetragonal form stable from 662°C to 769°C designated β uranium, and a body centered cubic (bcc) form stable from 769°C to 1133°C (melting point) designated γ uranium. The α phase is frequently dimensionally unstable during thermal cycling because of its anisotropic structure and its tendency to exhibit a preferred orientation. The phase is also dimensionally unstable under neutron irradiation, which renders it unsuitable as a nuclear fuel. These properties prompted the development of uranium alloys which would retain the isotropic γ phase at room temperature. In addition to improving dimensional stability, the γ alloys were found to have superior corrosion resistance and higher strengths than pure uranium.

Wilkinson[1] classifies uranium alloy systems as: (1) compound-free systems, (2) high γ-miscible systems, and (3) low γ-miscible systems with intermetallic compounds. Because of the desire to retain γ phase at low temperatures most of the development work has been done on high γ-miscible systems, primarily binary and higher-order alloys involving Mo, Nb, Zr, and Ti. Most of the work has been done on metastable uranium alloys quenched from the γ field.

Phase Transformations in Uranium Alloys

This discussion of phase transformations will be restricted to uranium-rich alloys, since the primary interest in alloying is to modify the phase transformations of pure uranium without substantially degrading the density or nuclear properties. The room temperature equilibrium structures of these materials consist of α uranium plus either alloy-rich solid solutions or intermetallic phases. On rapid cooling a series of metastable phases form martensitically. The structures that can occur when an alloy is quenched from the γ phase field are γ (the bcc phase is retained); γ^0 and γ^s, bct phases; α'', a monoclinic phase; and α', a distorted orthorhombic variant of α uranium. The differences in the crystal structures of the metastable phases are often subtle, and the lattice parameters change almost continuously with increasing alloy addition. The α' phase can have either an acicular martensite morphology or a banded morphology while the α'' phase has only the banded morphology. The γ^0 and γ^s phases appear similar to the γ phase metallographically and are based on a correlated displacement of average atoms and not on chemical order.[2] The transformation from γ to γ^0 or γ^s

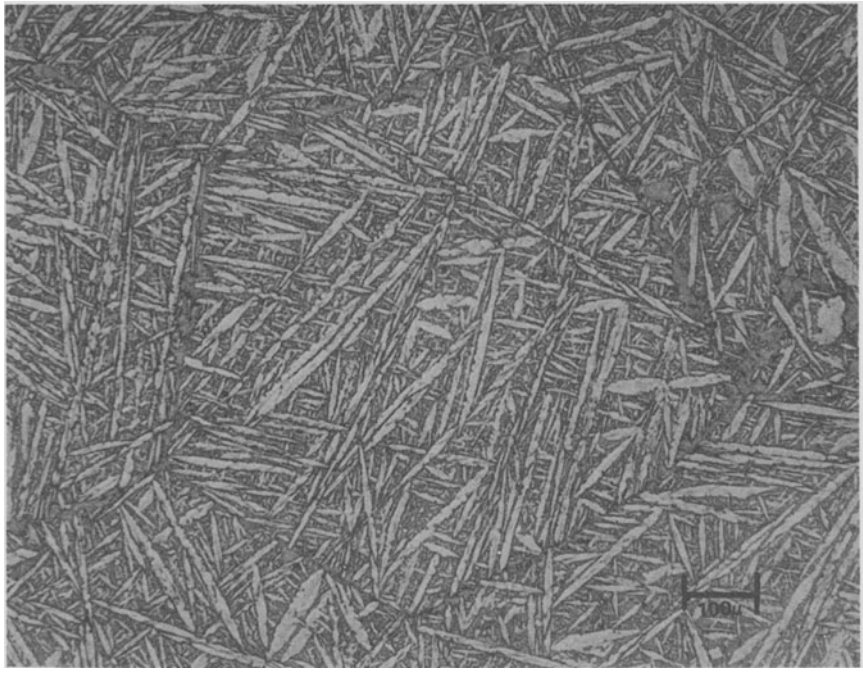

Fig. 1. Quenched U–0.75 % Ti with an acicular α' structure showing evidence of decomposition in the prior γ grain boundaries.

leads to a reduction in the number of nearest neighbors from 8 to 4, which is the number found in the other structures including α uranium. The acicular α' phase is shown in Fig. 1. Figure 2 shows the banded α' phase found in quenched U–2.25 % Nb.* Banded α'' has a similar appearance. The γ phase of quenched U–7.5 % Nb–2.5 % Zr is shown in Fig. 3. The metallographic structure is also representative of the γ^0 and γ^s phases.

The amounts of Mo, Nb, Zr, and Ti alloy additions needed to retain the γ-type phases in uranium during quenching as well as the amounts required to form the metastable α' and α'' phases are shown in Table 1. The principal goal of uranium alloy development programs has been isotropic, corrosion-resistant uranium. While only the γ-type phases are isotropic, the α' and α'' phases have higher strengths, better corrosion resistance, and better irradiation stability than pure uranium. The thermal cycling stability is also vastly improved as long as decomposition does not occur.

The alloy elements which are soluble in the γ uranium phase and have been used to stabilize this phase are essentially insoluble in α uranium.

* wt % will be used except where otherwise specified.

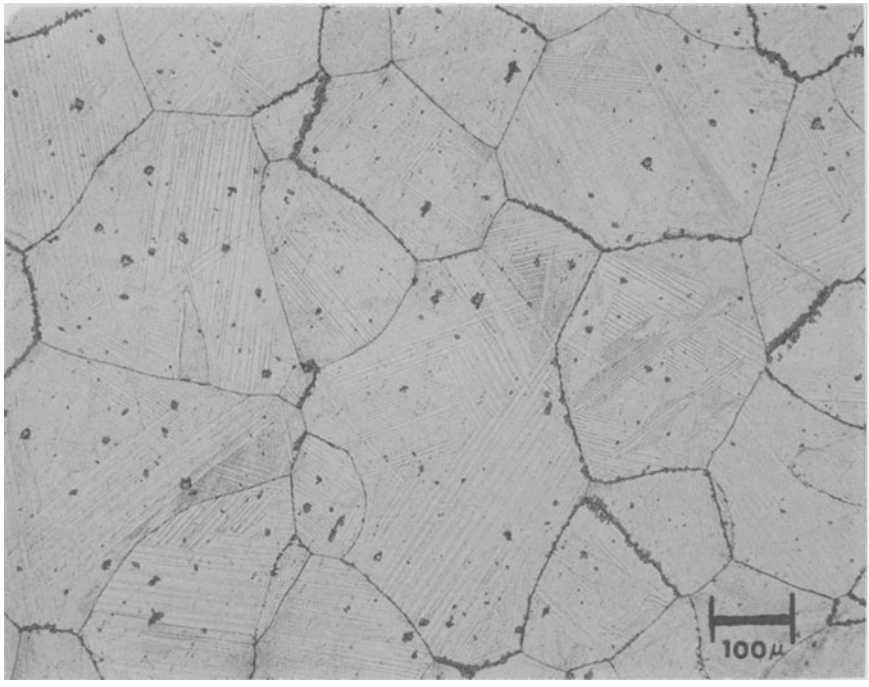

Fig. 2. Quenched U–2.25% Nb with a banded α'' structure showing evidence of decomposition in the prior γ grain boundaries.

Therefore, diffusional phase transformations forming almost pure α uranium and an alloy-rich γ phase will occur when the alloys are cooled slowly. These transformations allow the metastable alloys to be easily age hardened.[7] Initially on heat treating coherent precipitates form and strengthening occurs. If aging is continued, coherency is lost, the equilibrium phases are formed, and the strength of the alloys decreases. The precipitation of the

Table 1. Ranges of Metastable Phase Stability of Quenched Uranium Alloys

Alloy system	Reference	Phase		
		α'	α''	γ type
U–Mo	3	0.3–2.9%	3.0–4.6%	>4.8%
U–Nb	4	0.5–3.3%	3.8–6.5%	>7%
U–Zr	5	>6.4%	6.4–12.3%	>12.3%
U–Ti	6	>2.2%[a]	~2.3%[a]	>4.1%

[a] A two-phase α'' +. ^{0} phase forms in the U–Ti system in alloys with 2.6–3.2% Ti.

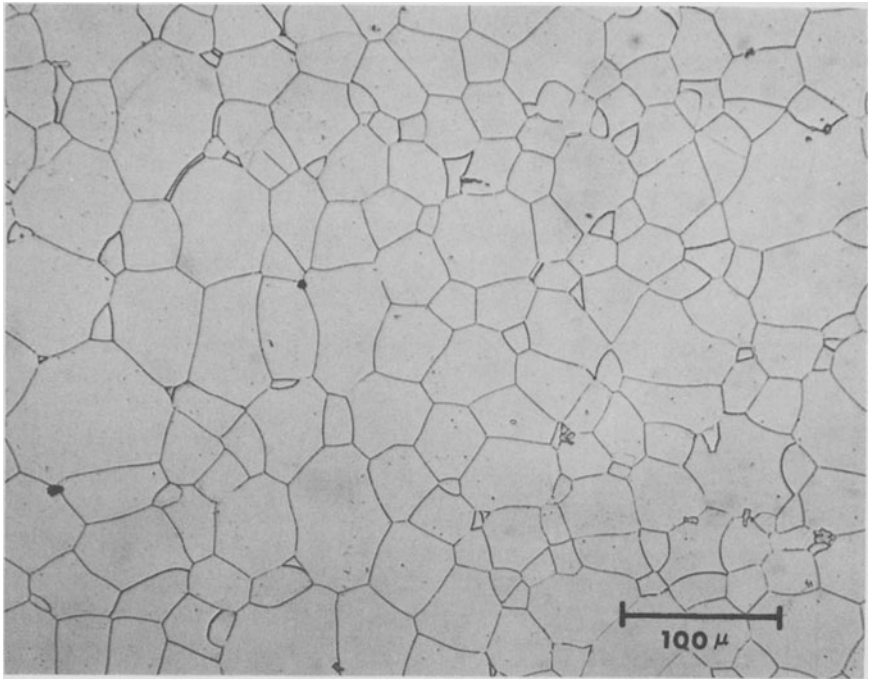

Fig. 3. Quenched U–7.5% Nb–2.5% Zr.

equilibrium phases occurs at grain boundaries and at inclusions in a classical manner.[7]

Embrittlement and Cracking Trends

While uranium and all of the uranium alloys that have been tested thus far are subject to environmental degradation, the behaviors are often not similar. The total range of alloy compositions that has been investigated ranges from pure uranium to alloys with 12% alloy addition, and can be divided into two groups. Pure uranium and alloys with up to a few percent alloy additions behave in one manner, while alloys with higher alloy contents behave in a different manner.

Pure uranium and the "lean" alloys are quite reactive and are degraded by H_2 and H_2O in the environment. While these materials are easily oxidized by O_2, they are not embrittled by or will not crack in O_2. The "rich" alloys are more corrosion-resistant and are more susceptible to stress corrosion cracking. With this type of alloy two types of stress corrosion cracking have been observed: intergranular cracking caused by an enhanced anodic

dissolution mechanism, and transgranular cracking caused by an oxide stress mechanism. The intergranular cracking requires H_2O, O_2 and Cl^-, initiates easily, and propagates rapidly. The transgranular cracking requires O_2, does not initiate easily, and propagates much more slowly than the intergranular cracking. These differences, particularly the ease of initiation, should be kept in mind because many of the seeming differences in the literature can be explained within the framework just discussed.

SYSTEMS THAT EMBRITTLE AND/OR STRESS CORROSION CRACK

Uranium

Internal H_2 Embrittlement

Uranium is an exothermic occluder of H_2 and reacts with H_2 to form UH_3. The calculated room temperature solubility of H_2 in α uranium is 0.00001 ppm,[8] (1 ppm by weight is equivalent to 0.024 at.%.) At higher temperatures the solubility increases but remains small. Cotterill[9] reports solubilities of 0.0006 ppm at 100°C, 2.2 ppm at 662°C (α-U), 7.8 at 662°C (β-U), 9.7 at 769°C (β-U) and 14.7 at 769°C (γ-U). The UH_3 that forms when these solubilities are exceeded has a density of $\sim 11\ g/cm^3$ compared to uranium, with a density of 19.1 g/cm^3. This corresponds to a 70% increase in volume when the hydride is formed. Because of the fast hydride nucleation rate and the low hydrogen solubility, a finely dispersed hydride forms which may not be observable by optical metallography.[8] Hydride precipitates have been reported in the grain boundaries of embrittled specimens,[10,11] but embrittlement has also been observed in specimens where no hydride precipitates could be found.[12]

Hydrogen in uranium increases the ductile to brittle transition temperature of uranium about 50°C from below room temperature to above room temperature[12] (Fig. 4). The figure also shows that above 100°C the embrittling effect of hydrogen disappears. Material tested below the ductile to brittle transition temperature exhibits primarily intergranular fracture, while material above the ductile to brittle transition temperature fails by microvoid coalescence.

Early mechanical properties studies on uranium showed that certain annealing media could have an embrittling influence on uranium but that the ductility could be restored by a vacuum anneal. The loss of ductility was

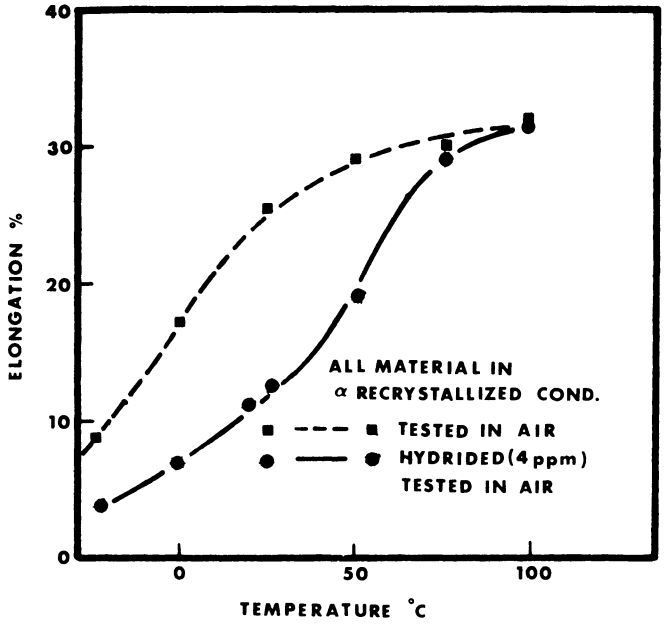

Fig. 4. The relationship between ductility and temperature for uranium (after Adamson, Orman, and Picton[12]).

attributed to hydrogen introduced into the metal during the salt bath anneal.[13] The data in Table 2 from Hanks *et al.*[13] show that small increases in the hydrogen contents are sufficient to cause embrittlement. Davis[14] reported that, for α and β annealed uranium, hydrogen did not change the shape of the stress–strain curve but did dramatically affect the ductility and the ultimate tensile strength. He found that 0.2–0.4-ppm hydrogen was sufficient to cause embrittlement and that increases in hydrogen concentration above 0.4 ppm had little or no further effect. Beevers and Newman[10] reported that embrittlement increased with H_2 content up to 2.5 ppm. However, the different hydrogen contents were produced by quenching from the α, β, and γ regions, and this could have affected the mechanical properties independent of the hydrogen levels. Powell and Condon[8] found that for both α and γ quenched uranium the ductility reached a lower plateau at $\sim$0.2 ppm H_2, Fig. 5. Adamson *et al.*[12] found for α recrystallized uranium a minimum in ductility occurred at 1–2 ppm in H_2, Fig. 6.

While the data in the literature show that hydrogen embrittles uranium, there is obvious disagreement as to the amount of hydrogen required, the magnitude of the effect, and the mechanism responsible. The differences in

Table 2. Room Temperature Properties of Uranium Containing Hydrogen[a]

Medium	Anneal Temperature,[b] °C	H_2, ppm	U.T.S., MN/m^2	Y.S. (0.2%), MN/m^2	%E, in 2 in.
Salt	600	1.50	793	279	4.5
Vacuum	600	0.50	917	324	21.6
Hydrogen	575	1.80	931	456	4.3
Vacuum	600	0.53	993	445	12.8
Salt	600	0.72	862	328	8.9
Vacuum	600	0.32	910	344	24.2

[a] After Hanks *et al.*, Ref. 13.
[b] 30 min at temperature.

the magnitude of the effect may be related to differences in the thermomechanical histories of the specimens used in the various investigations. These differences may also be partly due to differences in analysis techniques and hydrogen inhomogeneity. Hydrogen in uranium is often not homogeneously distributed, and it has been reported[8] that surface contaminants can greatly influence the hydrogen analysis. Davis[14] used previously analyzed

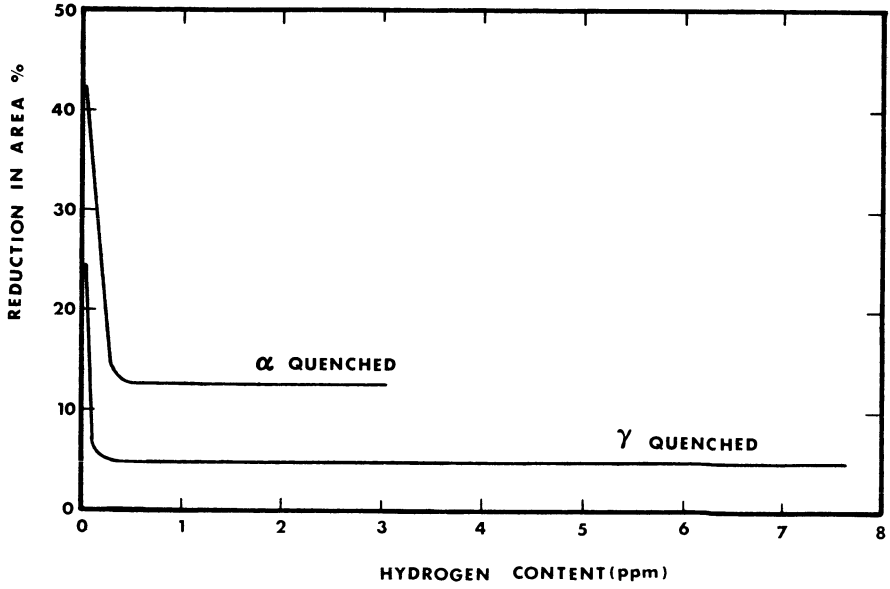

Fig. 5. The relationship between H_2 content and the ductility of α and γ quenched uranium (after Powell and Condon[8]).

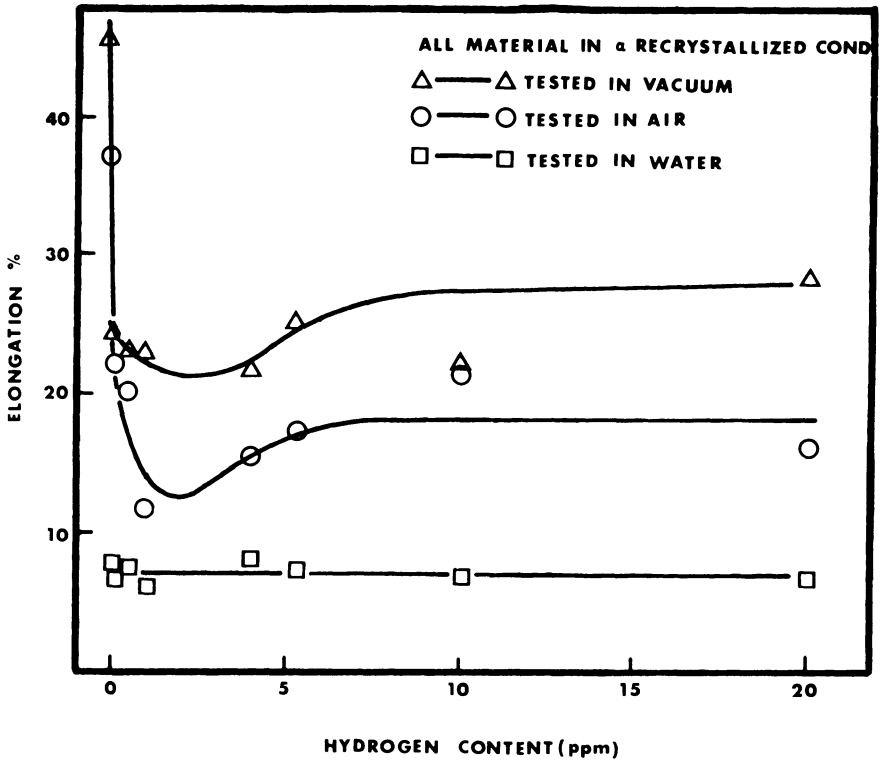

Fig. 6. The variation of ductility of uranium with hydrogen content (after Adamson, Orman, and Picton[12]).

uranium specimens as blanks to minimize the error caused by surface H_2 in the analysis, but even this cannot eliminate the possibility of errors in the <1-ppm range. The differences in the hydrogen concentrations required to cause maximum embrittlement, 0.2–2.5 ppm, may also be related in part to the levels of other impurities in the uranium. Uranium frequently has impurity contents of C, Fe, and Al greater than 100 ppm, and these impurities could alter the amount of hydrogen required for embrittlement. For example, it has been reported that there is a high solubility of hydrogen in UC at elevated temperatures which leads to preferential hydride precipitation at the inclusions on cooling.[15] Davis[14] observed that abnormally high absorption of hydrogen occurred at low hydrogen pressures (H_2 content of equilibrated specimens 0.2–0.4 ppm) which he felt was related to an impurity–hydrogen interaction which saturated at 0.4 ppm.

The embrittling effect of hydrogen in uranium can result from hydrogen in solution or as a hydride phase. Because of the extremely low solubility

of hydrogen in uranium the formation of a hydride phase is most likely to occur. Both the temperature dependence of the embrittlement, which shows the degree of embrittlement is the same at room temperature and $-78°C$,[9] and the strain rate dependence of the embrittlement, which shows embrittlement increases as the strain rate increases,[10] favor a brittle-phase mechanism over a solution mechanism. Beever and Newman[10] found that the maximum embrittlement occurred at the hydrogen concentration corresponding to the maximum length of grain boundary precipitates. Cotterill[9] postulated the occurrence of a grain boundary embrittling phase which would account for the saturation of the embrittling effect at a critical hydrogen concentration. The formation of this type of a phase would increase the effectiveness of the grain boundary as a dislocation barrier. Hence, the brittle–ductile transition temperature would be raised and the likelihood of intergranular fracture would increase, as has been observed.[8,12,14] The formation of a hydride phase, because of its relatively low density, could also lead to high internal stresses in the uranium which would contribute to the degradation of properties.

External Hydrogen

While hydrogen in the lattice has been shown to affect the mechanical properties of uranium, two investigations have found that gaseous hydrogen environments do not affect the properties.[12,16] However, the presence of an oxide film on the uranium in the static tests and impurities in the gases during both types of tests (there was no discussion in these investigations pertaining to either oxide removal or special gas cleaning precautions) are felt, by the author, to be responsible for the lack of an interaction.

Moisture can affect the mechanical properties of uranium. The data of Whitlow and Willows[16] in Table 3 show that H_2O (92% relative humidity) in air, O_2, or H_2 reduces the ductility of dynamically tested warm rolled uranium approximately 50% compared to 5% R.H. environments. The data also show that water immersion is even more deleterious than high relative humidities. Adamson *et al.*[12] have shown that water immersion is also worse than hydrogen in the metal, Fig. 6. The figure shows that while hydrogen in the metal lowers the ductility in both air and vacuum environments, the ductility under water immersion conditions is so low that no effect of internal hydrogen is observed.

Hughes *et al.*[17] reported that while moisture in the air affects the mechanical properties of uranium, certain conditions had to first be met. The conditions were (1) surface oxidation, specifically U_3O_8; (2) particular

Table 3. Tensile Properties of Warm-Rolled Uranium in Different Environments[a]

Environment	Relative humidity, %	U.T.S., MN/m^2	Elongation, %	Reduction of area, %
Vacuum	—	842	26	20
Air	5	842	22	18
	92	814	11	13
Oxygen	5	862	24	22
	92	787	11	12
Hydrogen	5	876	24	21
	92	807	12	13
Water (immersion)	—	787	7	8

[a] After Whitlow and Willows, Ref. 16.

metallurgical conditions, warm-worked or γ quenched; and (3) specimen shape, rectangular specimens and not circular cross-sectional specimens. However, the rectangular specimens had fine cracks prior to testing, while circular cross-sectioned specimens which were prepared by a different procedure did not. Therefore, it is doubtful that there is a shape sensitivity, but there is, rather, an initiation site sensitivity. In the presence of condensed water all conditions of uranium, with or without the U_3O_8 oxide, are embrittled.[18] These results indicate that the initiation process and not the propagation process is of critical importance to the embrittlement.

Hughes *et al.*[18] conducted mechanical properties tests in solutions as a function of pH and found that embrittlement only occurs over the pH range 5–10. The fact that embrittlement did not occur in the highly acidic environment was felt to indicate that the phenomenon is not related to the ingress of hydrogen. They proposed that the embrittlement is related to the oxidation of uranium and that the following reactions occurred at the metal surface:

$$H_2O \rightleftarrows H^+ \text{ (hydrated)} + OH^- \tag{1}$$

$$U \rightleftarrows U^{4+} + 4e \tag{2}$$

$$OH^- \rightarrow O^{2-} + H^+ \tag{3}$$

$$H^+ + e \rightleftarrows H \tag{4}$$

$$H + H \rightarrow H_2 \tag{5}$$

$$U^{4+} + 2O^{2-} \rightarrow UO_2 \tag{6}$$

At low pH (3) and hence (6) and (2) are retarded, while at high pH (4) and hence (2) are retarded. The loss of the embrittling effect at 100°C was felt to be due to slip occurring more easily and blunting the crack tip.

The fact that embrittlement does not occur in acidic solutions does not eliminate the possibility of embrittlement being due to hydrogen. Since the embrittling effect in water vapor[17] and in water[18] disappears at 100°C in a manner similar to that observed for internal hydrogen embrittlement,[12] it is felt that the same mechanism is operating. Another similarity between internal hydrogen embrittlement in uranium and embrittlement observed in H_2O is the fracture morphology. Predominantly intergranular cracking occurs in both types of embrittlement.[8,12,17,18] Uranium reacts with water vapor to form UO_2 and liberate hydrogen. Part of the hydrogen enters the gas phase, but part of the hydrogen is absorbed by the metal.[19,20] It is proposed that this hydrogen is responsible for the embrittlement observed in H_2O environments and that a mechanism similar to the internal hydrogen embrittlement mechanism is operative in this environment.

Uranium–Titanium Alloys

The effect of the environment on the mechanical properties of U–Ti alloys has only been determined for alloys with low Ti concentrations, 0.5 and 0.75%, and correspondingly high densities, 18.7 and 18.5 g/cm^3, respectively. These alloys behave in a manner similar to that of uranium: they are very reactive with the environment and are degraded by internal H_2 and H_2 or H_2O in the environment.

Environment

Internal H_2 embrittlement occurs in U–0.75% Ti, but the alloy is more tolerant of H_2 than pure uranium, and an order of magnitude more H_2 is required to produce embrittlement than is required for pure uranium.[8] Figure 7 shows the effect of hydrogen content on the ductility of quenched U–0.75% Ti; 1–2 ppm of H_2 decreases the reduction in area from 50% down to ~10%. Embrittlement has also been observed in humid environments.[21,22] Jackson[21] studied the effect of relative humidity from 0% (vacuum) to 100% (water immersion) on the strength and ductility of extruded U–0.75% Ti at strain rates of 0.005/min. The yield strength is not affected by the environment, but the ductility decreases with increasing relative humidity. Johnson *et al.*[22] obtained similar results. The elongation in a vacuum is 22% but decreases to only 2% in 100% R.H. air. Under immersion conditions embrittlement only occurs when the pH is between 2 and 12.[22]

Crack propagation tests conducted on U–0.75% Ti in O_2, H_2, and H_2O and tabulated in Table 4, show that H_2 and H_2O cause cracking but

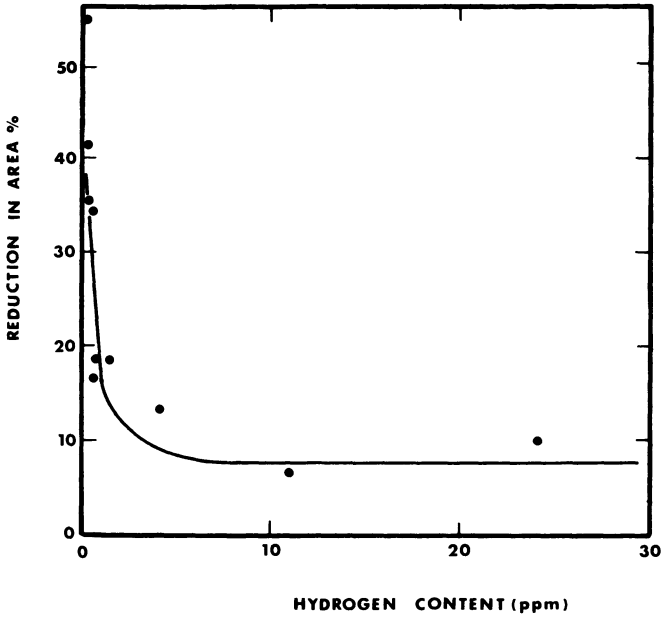

Fig. 7. The relationship between internal hydrogen concentration and ductility of quenched U–0.75% Ti (after Powell and Condon[8]).

O_2 does not. The U–Ti alloys react with H_2O very rapidly to form UO_2 and release H_2,[20] and therefore, cracking in H_2O and H_2 should be similar and caused by the same mechanism. Tests conducted in wet and dry air also showed water is the species responsible for cracking in laboratory air.[23] Results from the air tests and from tests conducted in 50-ppm Cl^- and $3\frac{1}{2}\%$ NaCl are shown in Fig. 8. The data show the threshold in dry air is only about 10% lower than the overload controls, while the threshold in the wet air

Table 4. The Effect of the Environment on the Time-to-Failure for Quenched U–0.75% Ti Loaded at 40 $MN/m^{3/2}$[a]

Environment	Time-to-failure, hr[b]
H_2O (23 Torr)	9
H_2 (100 Torr)	11
O_2 (150 Torr)	No crack growth in 1000 hr

[a] After Magnani, Ref. 23.
[b] Average of 2 tests.

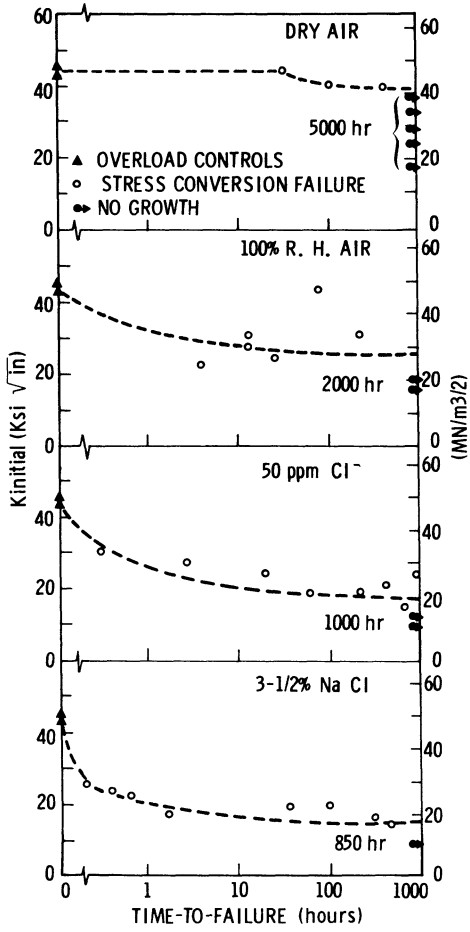

Fig. 8. The effect of the environment on the time-to-failure of U–0.75% Ti aged at 300 °C for 6 hr (after Magnani[23]).

is much lower, and that K_{ISCC} is not dependent on Cl^- concentration. The lack of dependence of K_{ISCC} on Cl^- concentration indicates that this species does not play a dominant role in the cracking process as it does with the heavily alloyed materials. Crack propagation tests were also conducted in a vacuum to confirm that the dry-air failures are not due to a stress rupture mechanism.[23] K_{ISCC} in a vacuum is about that observed in the 100% R.H. air tests and much lower than that observed in dry air. Crack

velocity studies showed that cracking in pure H_2O or H_2 is inhibited by adding O_2 to the system. This suggests that the vacuum failures were caused by water which was not removed from the vicinity of the crack tip and that the high K_{ISCC} in dry air was due to O_2 inhibition. (K_{ISCC} = plane strain threshold for stress corrosion crack propagation.)

Tests conducted in H_2 show that crack propagation occurs at very low stress intensities and continues when the applied load is completely removed from the specimen.[24] This cracking is attributed to hydride wedging in the vicinity of the crack tip. Figure 9 shows a crack with the hydride corrosion products wedging the specimen open. The corrosion products ignited when air was introduced into the system, also suggesting UH_3 was formed.

The U–0.5% Ti alloy has been tested in ~10% R.H. air and in 50-ppm Cl^-[25]. The alloy is more susceptible to cracking in 10% R.H. air than the 0.75% Ti alloy is in desiccated air, but this is attributed to the higher relative humidities in the 0.5% tests. Quenched U–0.5% Ti tested in 50-ppm Cl^- has a K_{ISCC} of 24 $MN/m^{3/2}$, which is about half of the overload value.

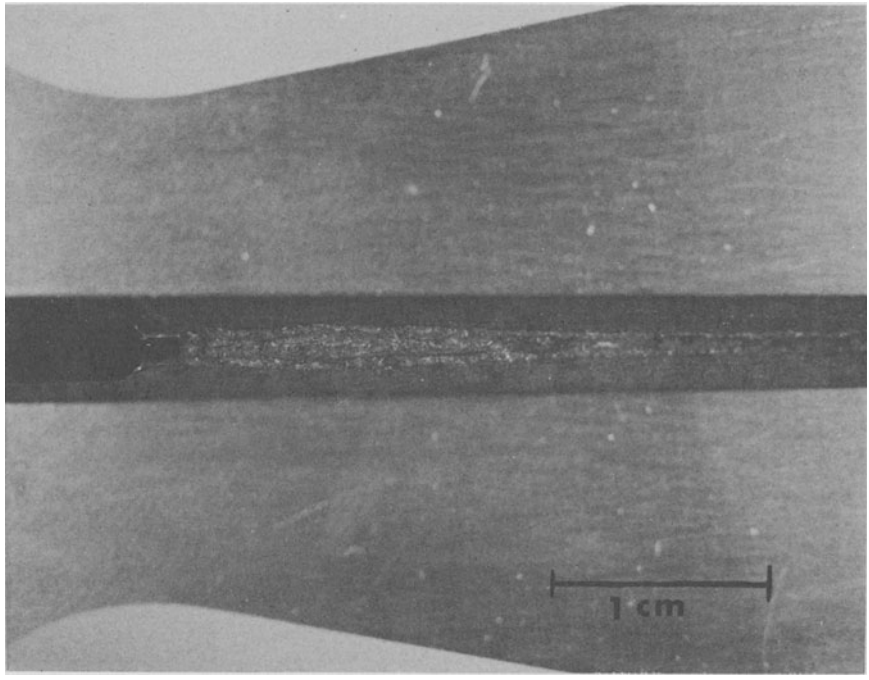

Fig. 9. Corrosion products wedging a crack open in U–0.75% Ti. Environment 100 Torr of H_2 (3×).

Heat Treatments

McLaughlin and Stephenson[26] studied the effect of heat treatment on crack initiation in U–0.5% Ti in Cl^- solutions. They aged specimens at temperatures from 200 to 700°C for times of 2, 8, 24, and 80 hr. Their data show that material aged at 400°C, irrespective of the time, is the most susceptible to cracking, while the 600°C material is the most resistant. The overaged 600°C material forms a two-phase mixture of $\alpha + U_2Ti$, while the most susceptible material does not decompose into the equilibrium phases, but shows evidence of G.P. (Gruinier–Preston) zone formation (pre precipitates).

The U–0.75% Ti alloy has also been tested with several different heat treatments. The results of tests conducted in 50-ppm Cl^- on specimens in the quenched condition (704-MN/m^2 yield), quenched and aged at 357°C for 18 hr (880-MN/m^2 yield), and quenched and aged at 400°C for 42 hr

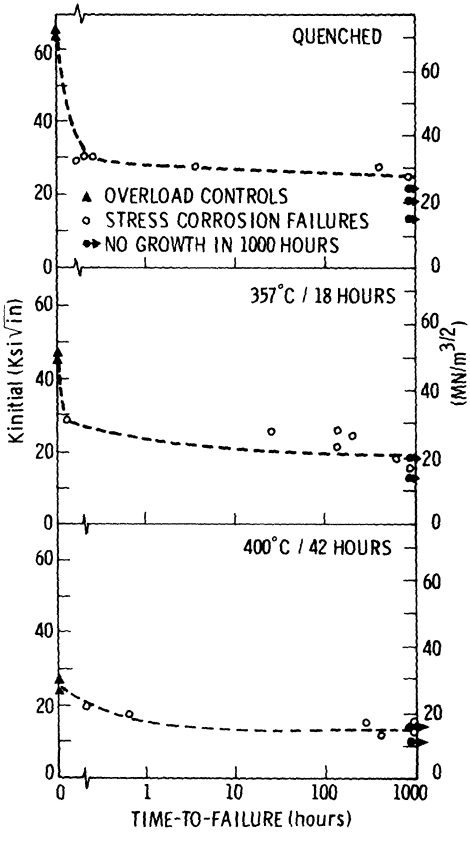

Fig. 10. The effect of heat treatment on time-to-failure of U–0.75% Ti tested in 50-ppm Cl^- (after Magnani[23]).

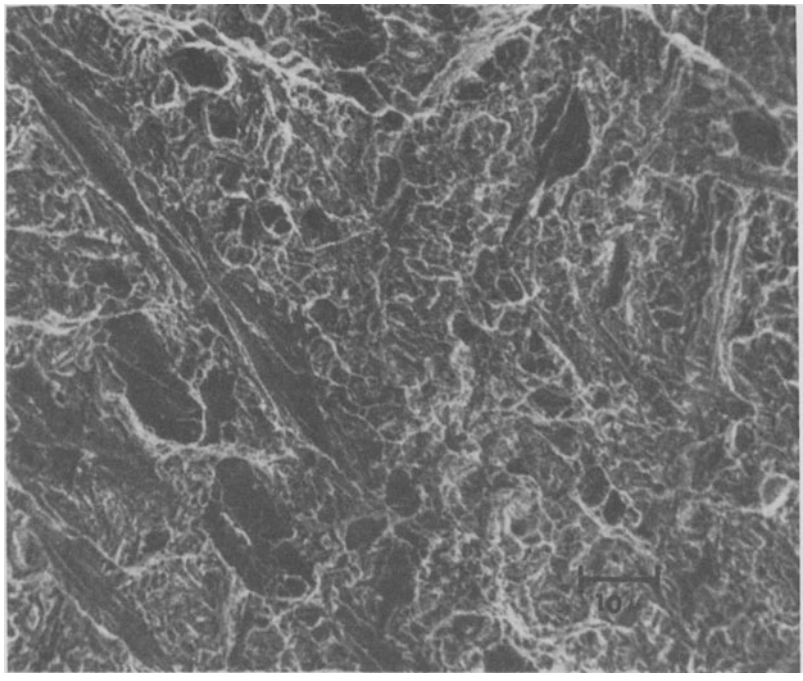

Fig. 11. Slow crack growth in U–0.75 % Ti aged at 357 °C for 6 hr and tested in 50-ppm Cl^-, 3-ppm H_2 in the metal.

(1110-MN/m^2 yield) are shown in Fig. 10. The data show that as the strength increases, K_{ISCC} decreases from 28 to 21 to 14 MN/m$^{3/2}$. The differences in threshold are attributed to differences in strength level since the microstructural changes are not very great. In fact the degree of environmental degradation in all of the conditions is 50 % of the overload stress intensity, indicating the importance of the nonenvironmental properties.

Czyrklis and Levy[27] tested extruded U–0.75 Ti in H_2O (<1 ppm Cl^-) and in $3\frac{1}{2}$ % NaCl. They obtained K_{ISCC} values of 23 MN/m$^{3/2}$ and 17 MN/m$^{3/2}$ in the Cl^- free and Cl^- environments, respectively, for the 607-MN/m^2 yield material. Tests conducted on extruded material aged at 450°C for 4 hr (1075-MN/m^2 yield) show that K_{ISCC} is 15 MN/m$^{3/2}$ in the H_2O environment and 11 MN/m$^{3/2}$ in the $3\frac{1}{2}$ % NaCl environment.[28] Similar material was also tested in 100 % R.H. air and in 50-ppm Cl^- solutions.[29] K_{ISCC} is 18 MN/m$^{3/2}$ in the air environment and 11 MN/m$^{3/2}$ in the Cl^- environment. These data show again that Cl^- concentration does not strongly affect K_{ISCC} for U–0.75 % Ti.

Fractography

Stress corrosion fracture in U–0.50[26] and in U–0.75% Ti[20,22,23,27,29] alloys is transgranular. Intergranular fracture along prior γ grains has not been reported. Figure 11 shows a U–0.75% Ti fracture surface of an extruded specimen aged at 357°C for 18 hr and exposed to 50 ppm Cl^-; a great deal of dimpling occurs on the surface. In extruded material with a lower H_1 content (0.3 ppm versus 3 ppm) the fracture surface is composed of a mixture of cleavage and quasi-cleavage, Fig. 12. The environment does not affect the fracture mode in either type of material; fractures in dry air, wet air, and Cl^- solutions are identical.[23] The strength level of the material also does not affect the fracture surface.[23]

Summary

U–Ti alloys with low Ti concentrations are susceptible to internal H_2 embrittlement and to embrittlement by moisture in the environment in a

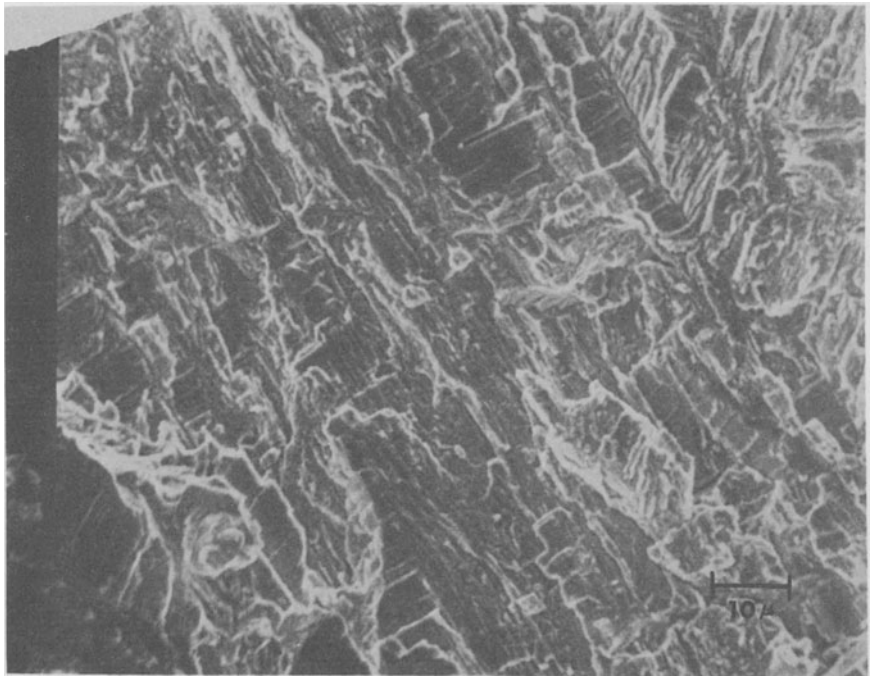

Fig. 12. Slow crack growth in U–0.75% Ti aged at 380°C for 6 hr and tested in 100% R.H. air, 0.3-ppm H_2 in the metal.

manner similar to that of pure uranium. Additionally, the U–Ti alloys stress corrosion crack in H_2 and H_2O. The cracking and embrittlement are both attributed to the formation of UH_3. Oxygen inhibits crack propagation in these alloys presumably by the same mechanism by which it inhibits hydriding.

The data show that for underaged alloys the susceptibility is inversely related to the strength of the alloy, and that overaged alloys are more resistant to cracking than underaged alloys. Stress corrosion crack propagation is transgranular for all of the heat treatments and there is no evidence of cracking along the prior γ grain boundaties.

Uranium–Molybdenum Alloys

One of the first indications that the environment degraded the properties of uranium alloys was the disintegration of U–Mo oxidation specimens observed by Burkart, Cohen, and McGeary.[30] They attributed the disintegration in 315°C water to the formation of hydride platelets in the γ matrix and the subsequent oxidation of the hydride by H_2O. While this was the first type of failure reported in uranium alloys, it is not related to the latter failures observed in U–Mo at room temperature.

Hills, Butcher, and Howlett[5] determined the mechanical properties of quenched uranium alloys with Mo contents from 0.6 to 13% and found that many of the specimens had extremely low ductilities in laboratory air. The low ductility and circumferential cracking observed in specimens with 2.5–7.0% Mo were attributed to stress corrosion cracking. Figure 13 compares a U–5% Mo specimen tested in laboratory air with one tested in a vacuum. Hills *et al.*[5] also found that specimens containing more than 9% Mo were brittle, but this was not attributed to stress corrosion cracking because high ductilities occur at low strain rates. Instead, the intergranular cracking was attributed to grain boundary precipitates (presumably hydrides).

It should be noted that the majority of the work on U–Mo alloys has been conducted on relatively corrosion-resistant γ alloys, and therefore the alloys do not behave in a manner similar to that observed in uranium or U–Ti alloys.

Environment

While there is general agreement in the literature that the reduction of ductility observed in U–Mo alloys at low strain rates is due to stress corrosion cracking and not hydrogen embrittlement, there is some disagreement as to

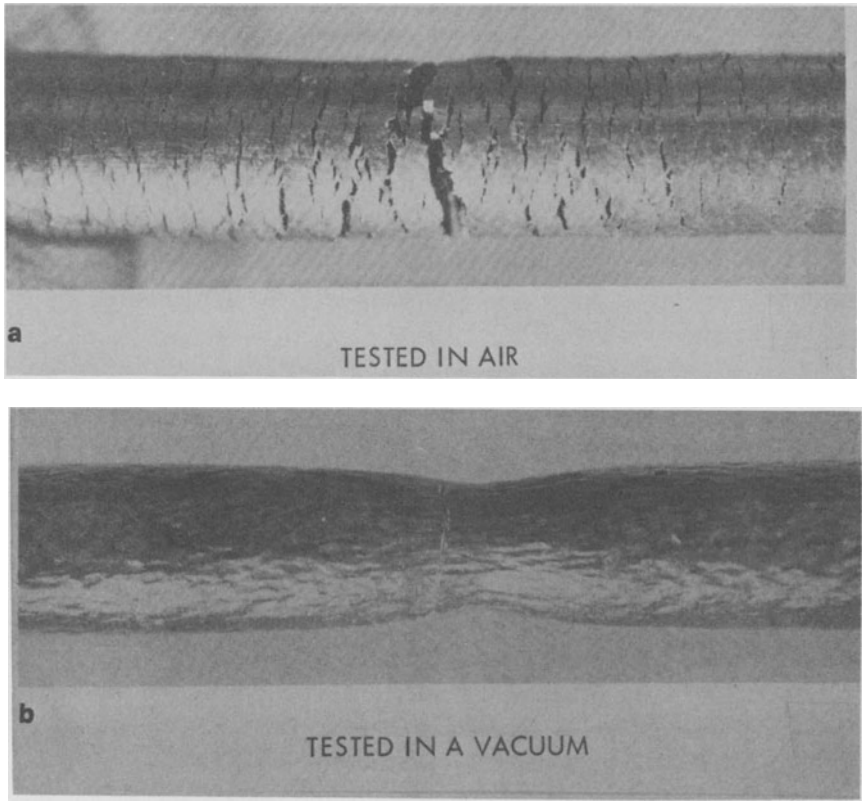

Fig. 13. The surfaces of quenched U–5% Mo tensile specimens tested in air (a) and in a vacuum (b) (after Pridgeon[31]).

which gaseous specie(s) in the air is responsible for the cracking and loss of ductility. The majority of the investigations reported in the literature show that cracking occurs in O_2, but some of the data also show that other gaseous species are harmful.

Peterson and Vandervoort[32] studied the effect of the environment on the tensile properties of U–10% Mo, the most extensively studied U–Mo alloy, and concluded that O_2 is responsible for the cracking and loss of ductility. Their data in several environments are shown in Table 5. In addition to showing O_2 is responsible for the loss in ductility, the data show that 50% R.H. air is less aggressive than dry air. This is attributed to condensed water in the cracks denying easy access of O_2 to the crack tip. However, Hoenig and Sulsona[33] found that O_2, H_2, and H_2O could lead to reductions of ductility in the same alloy. Pridgeon[31] showed that O_2 cracks U–4% and U–5% Mo alloys.

Table 5. The Ductility of U–10 wt% Mo in Various Environments[a]

Environment	Elongation,[b] %
Vacuum	19.0
50% R.H. air	5.0
Dry air	1.3
Dry N_2	19.3
Dry O_2	1.2
Dry CO_2	20.0

[a] After Peterson and Vandervoort, Ref. 32.
[b] $\dot{\varepsilon}$ = 0.0005/min.

Both dynamic and static tests were used by Orman and Picton[34] to identify the species responsible for cracking in U–7.5% and U–10% Mo alloys. Their data show that the U–7.5% alloy is more susceptible to cracking and cracks in air, O_2, and H_2O. The authors proposed that an acidic gas in the air is responsible for cracking in the U–10% alloy, but they were not able to duplicate the results in mixtures containing CO_2, SO_2, or NO_2.

The bulk of the reported data on U–Mo stress corrosion cracking have been obtained using smooth specimens, but two investigations have used precracked specimens and a fracture mechanics analysis.[25,35] Figures 14 and 15 show the results of time-to-failure tests conducted on U–10% Mo with 15-ppm C and tested in < 10% R.H. air and 100% R.H. air, respectively. The

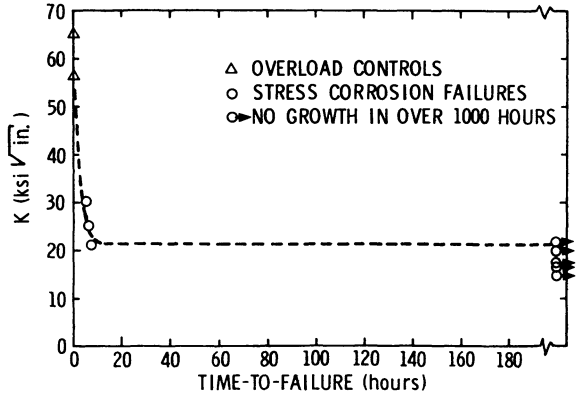

Fig. 14. The effect of the initial stress intensity on the time-to-failure for quenched U–10% Mo tested in dry air (< 10% R.H.) (after Magnani[25]).

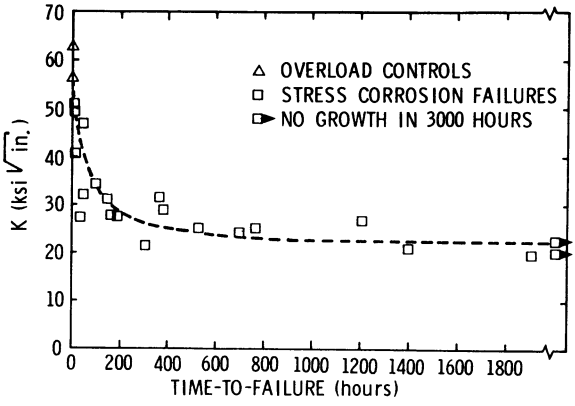

Fig. 15. The effect of the initial stress intensity on the time-to-failure for quenched U–10% Mo tested in 100% R.H. air (after Magnani[25]).

figures show that K_{ISCC} is $\sim 22\ MN/m^{3/2}$ for both environments but that the time-to-failure is very short in the dry air compared to wet air. Nomine *et al.*[36] found that the incubation times are only a small fraction of the times-to-failure even at low stress intensities, Fig. 16. This suggests that the shorter failure times in dry air are due to faster crack propagation.

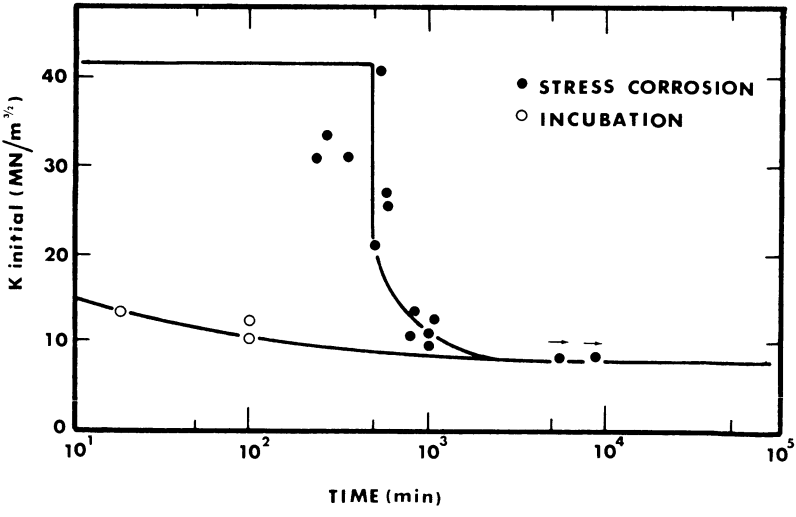

Fig. 16. The incubation time and time-to-failure for quenched U–10% Mo tested in laboratory air (after Nomine *et al.*[36]).

Strain Rate

The effect of strain rate on the embrittlement and cracking in U–Mo alloys has been studied by several investigators. The critical strain rate (the strain rate giving the maximum ductility) for U–10% Mo has been reported between 0.03/min and 0.12/min.[32,35–38] The relationship between strain rate and elongation for one of the investigations is shown in Fig. 17. The data show that above ~0.03/min the ductility is independent of environment, but below 0.03/min the ductility decreases to almost zero at 0.0001/min in laboratory air but remains relatively unchanged in a vacuum.[32] Nomine *et al.*[35] related the reduction of ductility to the percent of the fracture surface which stress corrosion cracked. Figure 18 shows their results. The data show

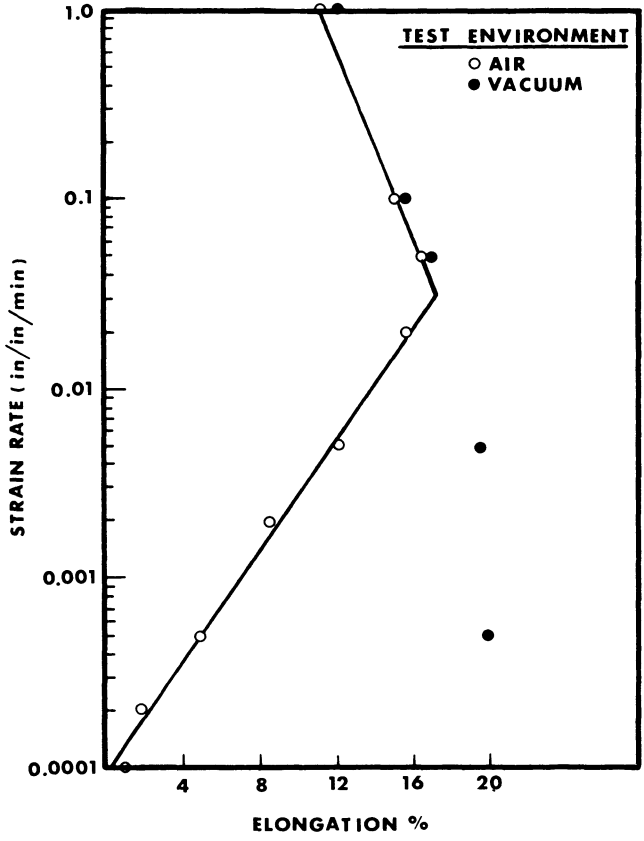

Fig. 17. The effect of strain rate on the ductility of U–10% Mo (after Peterson and Vandervoort[32]).

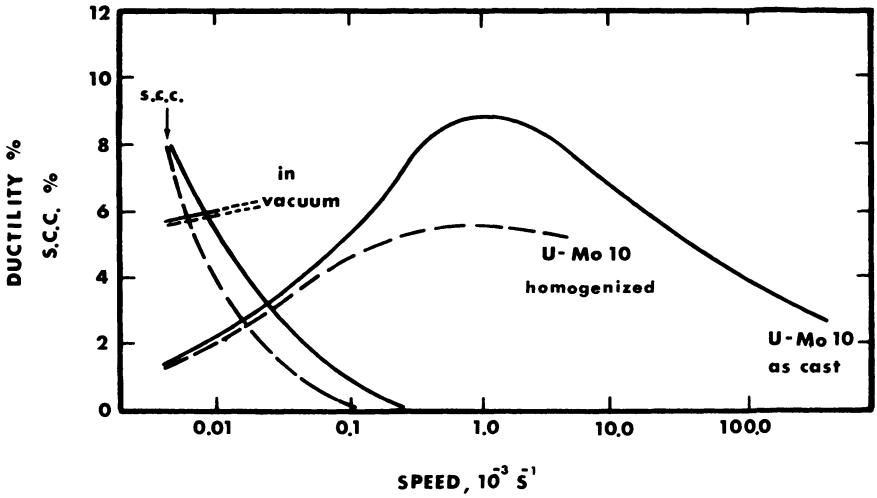

Fig. 18. The effect of strain rate on ductility and stress corrosion cracking in quenched U–10% Mo (after Nomine, Bedere, and Miannay[35]).

that as ductility increases to its maximum stress corrosion cracking goes to zero. Pridgeon[31] found that the critical strain rate for the U–5% alloy was much higher, 10/min, than any of the values reported for the U–10% Mo alloy.

Alloy Chemistry

The data of Orman and Picton[34] and Pridgeon[31] indicated that lower Mo contents lead to more susceptible alloys. Nomine *et al.*[35] tested alloys with 8, 10, and 12% Mo and found a similar behavior, see Table 6. In fact, the 12% alloy is not susceptible to stress corrosion cracking in the homogenized condition and the cast 12% alloy is susceptible only in Mo-depleted regions. However, the 12% alloy is very brittle and cannot be considered a good engineering material. The data in Table 6 also show that little is gained by substituting Ti for Mo and that the substitution of Zr for Mo leads to an even more susceptible alloy.

Several other alloy additions to U–Mo have been made to reduce the susceptibility to stress corrosion cracking without any success. The substitution of Nb for Mo in a U–8% Mo–2% Nb alloy lead to a more susceptible alloy than the U–10% Mo alloy.[32] Willows and Whitlow[39] added small quantities of Si and Sn to a 5% alloy and still observed cracking in dynamic tests.

Table 6. K_{IC} and K_{ISCC} of Several U–Mo Alloys[a]

Ingot Comp.[b]		K_{IC}, MN/m$^{3/2}$	K_{ISCC}, MN/m$^{3/2}$
U–8 wt % Mo	Cast	40.5	6.2
	Homogenized	37	4.5
U–10 wt % Mo	Cast	34.3	13.5
	Homogenized	35.5	7.5
U–12 wt % Mo	Cast	28.6	18
	Homogenized	23.5	Not susceptible
U–8 wt % Mo–1 wt % Ti	Cast	44.1	10.5
	Homogenized	66.3	7.5
U–10 wt % Mo–1 wt % Zr	Cast	45	7.5
	Homogenized	50.6	6

[a] After Nomine *et al.*, Ref. 35.
[b] 100–200-ppm C.
[c] Lab air tests.

Carbon content has been found to have a pronounced effect on the cracking susceptibility of U–Mo alloys. Peterson and Vandervoort[32] studied the effect of carbon content on the cracking behavior of U–Mo alloys. They found the threshold for cracking increased from 260 MN/m^2 to 605 MN/m^2 when the carbon content was decreased from 408 to 65 ppm. This improvement led to the addition of Ti to U–Mo alloys to scavenge the carbon and float it to the top of the melt to thus reduce the carbon content. An 8 % alloy with 1 % Ti had a carbon content of only 15 ppm and a threshold for cracking of 745 MN/m^2.[32] Another alloy with the same Mo content, with only half as much Ti and 75-ppm C had a threshold of 425 MN/m^2.[37] These data indicate that the carbon level is the more important variable than the Ti content. The differences reported for K_{ISCC} for the 10 % Mo alloy in laboratory air[25,36] may also be due to the differences in carbon content.

Heat Treatment

Some improvement in reducing susceptibility to cracking has been obtained by heat treatment. The bulk of the work on U–Mo alloys is on alloys quenched to retain the γ structure. When these alloys are heat treated to form the equilibrium $\alpha + \gamma$ phases they are much more resistant to stress corrosion cracking.[37,40] Hoenig and Sulsona[33] reported that an alloy (U–10 % Mo) quenched and aged at 300°C for 24 hr had α precipitates present but had a threshold for cracking of only 255 MN/m^2, indicating that partially transformed material is still susceptible to cracking.

Fracture Morphology

There is good agreement in the literature concerning the fractography of stress-corroded U–Mo specimens. Macroscopically a tarnished surface is observed where stress corrosion cracking has occurred. Microscopically the fracture mode of the stress corrosion cracking observed in air and in O_2 is transgranular[25,31,34,35,37,40] and reported in one investigation to occur on $\{111\}_{\gamma^0}$ planes.[35] Figure 19 shows a U–10% Mo transgranular quasicleavage fracture surface. Whitlow found that in overaged U–6% Mo cracking occurs along the prior γ grain boundaries while quenched material cracks transgranularly. Intergranular stress corrosion cracking was also observed in quenched materials tested in aqueous solutions.[25,36]

Summary

U–Mo alloys are susceptible to both embrittlement and stress corrosion cracking in laboratory air. However, contrary to the behavior observed with uranium and U–Ti alloys, O_2 is primarily responsible. This is related to the

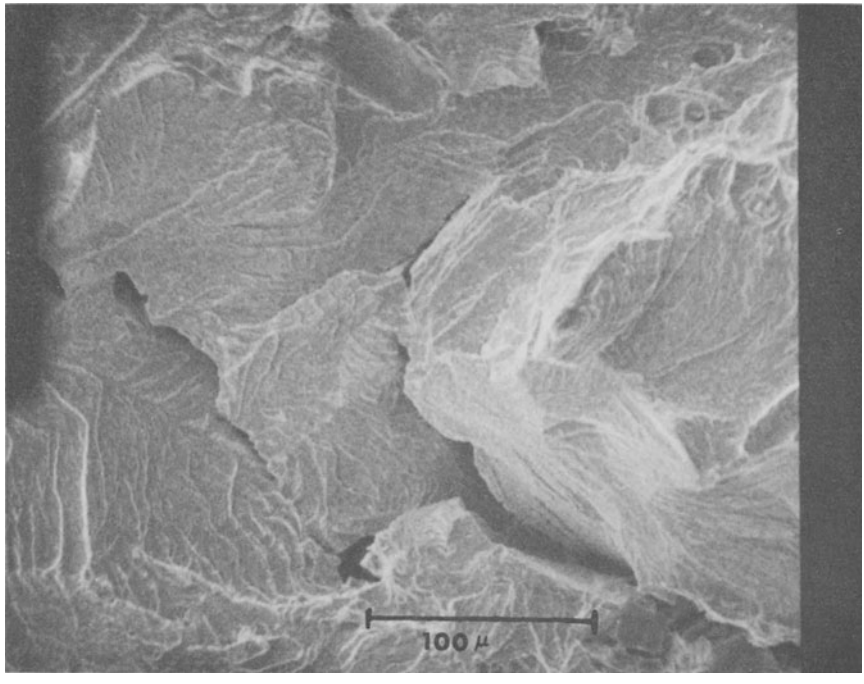

Fig. 19. Quasicleavage fracture in quenched U–10% Mo tested in laboratory air.

higher alloy levels of the U–Mo alloys that have been tested and not to a fundamental difference in alloying behavior. The carbon content is important to the cracking behavior, higher carbon alloys being more susceptible. Alloys with lower Mo contents are also more susceptible to cracking. Heat treating quenched alloys can lead to significant improvements in stress corrosion resistance in that alloys with equilibrium microstructures are much more resistant to cracking than metastable alloys. However, this type of treatment leads to some deterioration in corrosion resistance and some loss of strength.

Uranium–Niobium Alloys

The effects of the environment on the mechanical properties of U–Nb alloys have been determined for alloys with 2.3–8.5% Nb (the actual compositions studied are 2.3%, 4.2–5%, 6%, and 8.5%). The 2.3% Nb alloy is reactive and exhibits some of the characteristics of U and U–0.75% Ti. The alloys with higher Nb concentrations such as the 6% and 8.5% alloys behave in a manner similar to that of U–Mo alloys, while alloys with a Nb concentration of about 4.5% Nb exhibit some of the characteristics of both types of behavior.

The U–8.5% Nb alloy is the only U–Nb alloy in which the effect of internal hydrogen has been determined. Powell and Condon[8] found that the ductility of this material decreased from 50% R.A. in a hydrogen-free condition to 1% R.A. with 15 ppm of internal H_2. Further increases in H_2 content did not affect the ductility.

Environment

The U–2.3% Nb alloy is the only U–Nb alloy which has been reported to be embrittled by humid environments. Zehr[41] found that while the 2.3% Nb alloy is embrittled in several heat-treated conditions, the material in some conditions still has reasonable ductilities. He reported elongation in $\alpha + \gamma$ material of 40%, 25%, and 16% for vacuum, 50% R.H. air, and water immersion, respectively.

The lack of data indicating reductions in ductility in other U–Nb alloys in humid test conditions may be due to the reduced reactivity of the alloys as the Nb concentration is increased. Tests conducted in 100% R.H. air at 75°C show that the 4.5% Nb alloy reacts with water vapor about one order of magnitude more slowly than the 2.3% alloy and that the 6 and 8.5% alloys are even less reactive than the 4.5% alloy.[20] Crack propagations studies on

U–4.5% Nb show that stress corrosion cracking can occur in wet N_2,[42] while similar studies on the U–6% Nb alloy show that cracking will not occur in H_2O.[43] This behavior is also attributed to the relative reactivity of the alloys.

Macki and Kochen[44] have reported that Cl^-, O_2, and H_2O may be required for stress corrosion crack initiation in U–4.2% Nb. Some of their data are shown in Table 7. The data show that four-point bend specimens loaded at 900 MN/m^2 in dry air and in 100% R.H. air did not fail in 10,000 hr, while specimens in oxygenated 50-ppm Cl^- solutions failed in 2–5 hr. At lower stresses, 345 MN/m^2, tensile specimens tested in Cl^--free solutions failed in 2400–4000 hr, and the addition of Cl^- (50 ppm) reduced the times to 1–8 hr. The substitution of N_2 for O_2 gave mixed results with the failure time ranging from 7 to 1000 hr. The authors speculated that O_2 contamination caused the shorter failure time.

More recent tests on the 4.5% alloy have shown that crack propagation occurs in O_2 and in H_2O.[45] A synergistic interaction occurs in mixtures of the gases, and crack propagation is significantly higher than would be expected from the data for the pure gases. Tests conducted in various pressures of O_2 show that the crack velocity decreases and K_{ISCC} increases as the O_2 pressure is decreased. The data are shown in Fig. 20.

Crack propagation tests have also shown that Cl^- has very deleterious effects on the U–4.5% Nb alloy.[46] Specimens loaded at 33 $MN/m^{3/2}$ failed in ~270 min in distilled water and in 3–15 min in 5-, 25-, and 50-ppm Cl^-, while only 1 min was required for failure in 500-ppm Cl^-. The thresholds for stress corrosion cracking K_{ISCC} were not strongly affected by the Cl^- concentration, however.[25] For the <2-, 5-, 25-, and 50-ppm Cl^- solutions

Table 7. The Results of Four-Point Bend Tests and Static Tensile Tests on U–4.2 wt% Nb Aged 80 hr at 260°C[a]

Load, Mn/m^2	Environment	Time-to-failure, hr
	Four-point bend tests	
900	Dry air	>10,000
900	100% R.H. air (32°C)	>10,000
900	O_2–H_2O–Cl^-(50 ppm)	2 → 5
	Static tensile tests	
345	O_2–H_2O (Cl^- ≃0.5 ppm)	2400 → 4000
345	O_2–H_2O–Cl^-(50 ppm)	1 → 8
345	N_2–H_2O–Cl^-(50 ppm)	7 → 1000

[a] After Macki and Kochen, Ref. 44.

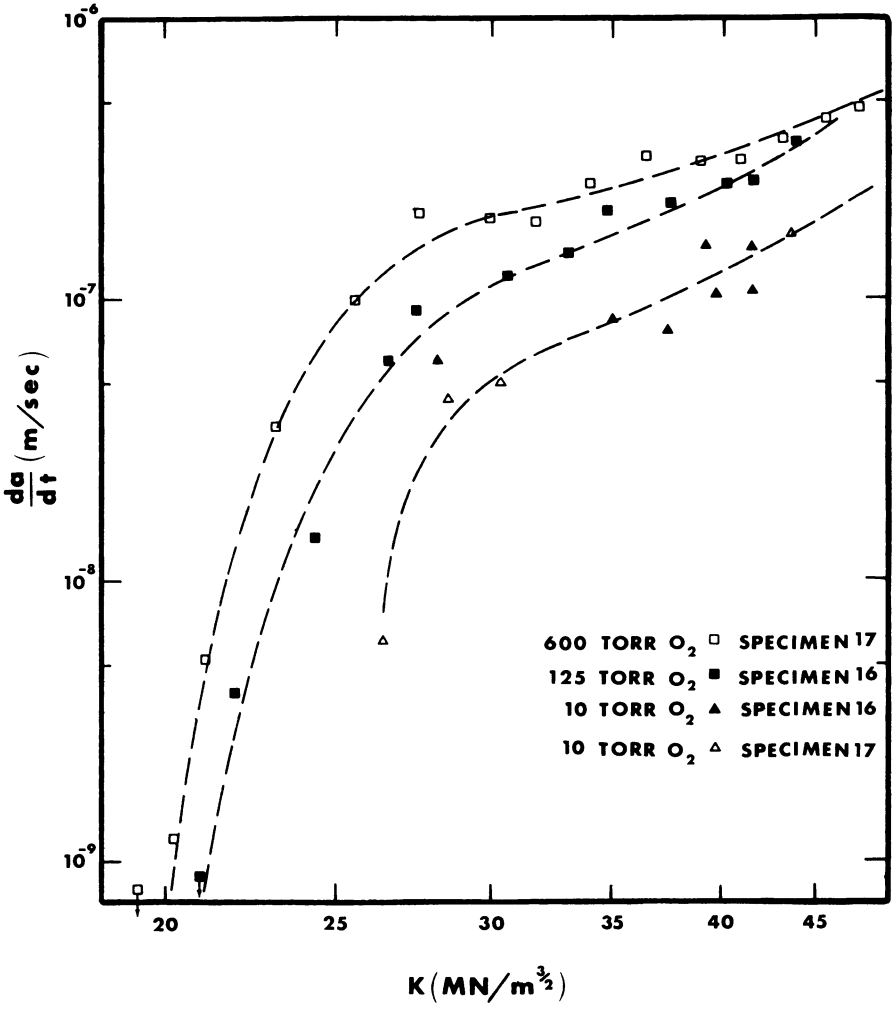

Fig. 20. The stress corrosion crack velocity of U–4.5% Nb aged at 260 °C for 80 hr and tested in oxygen with 2-Torr H_2O (after Magnani[45]).

K_{ISCC} was between 17 and 22 MN/m$^{3/2}$. The threshold based on 1000-hr tests, in 500-ppm Cl^- was ~16 MN/m$^{3/2}$, but cracking occurred even in unloaded specimens after very long times. This cracking was attributed to corrosion product wedging.

The U–2.3% Nb and U–6% Nb alloys have been tested and found to crack in pure H_2 environments.[43] It is assumed cracking will also occur in the other U–Nb alloys in H_2 environments. Table 8 shows the results of the

Table 8. U–6Nb Stress Corrosion Cracking in Pure Gases[a]

Environment	Pressure Torr	K $MN/m^{3/2}$	Time-to-failure, hr
O_2	150	37	91
O_2	150	36	71
H_2	150	36	70
H_2	150	38	78
H_2O	25 (100% R.H.)	36	1680 (no growth)
H_2O	25 (100% R.H.)	38	1010 (no growth)
N_2	650	35	1780 (no growth)
N_2	650	36	1610 (no growth)

[a] After Magnani, Ref. 43, material as-quenched.

U–6 Nb H_2 tests and of tests in O_2, H_2O, and N_2 showing that this alloy is susceptible to cracking in O_2 and H_2 but not in N_2 or H_2O. This behavior is similar to that of the U–Mo alloys.

Heat Treatment

2.3 Nb. Very little information has been reported in the literature on the effect of heat treatment on the cracking behavior of U–2.3% Nb. Macki and Kochen[47] tested the alloy in an underaged condition (230°C for 24 hr), and in an overaged condition (430°C for 24 hr), both of which produce material with a 930-MN/m^2 yield strength. The data show that the underaged material with an α' structure is more susceptible to cracking than the overaged material with an $\alpha + \gamma_2$ structure. The tests, conducted in 50-ppm Cl^- at 230 MN/m^2, yielded failure times of 1300–2900 hr for overaged material compared to 180–390 hr for the underaged material. Miller[48] tested the 2.3% alloy in two overaged conditions, 455°C for 35 hr (830-MN/m^2 yield) and 600°C for 5 hr (550-MN/m^2 yield), in 100% R.H. air. His data show that K_{ISCC} is approximately the same for both of the overaged conditions, 20 $MN/m^{3/2}$ and 22 $MN/m^{3/2}$, respectively.

4.5–5% Nb. The U–4.5 wt% Nb alloy has been tested in several different aging conditions, with the most common a 260°C–80 hr age. The alloy in the quenched condition has the same K_{ISCC} for both wet and dry air, 22 $MN/m^{3/2}$.[25] In the 260°C–80 hr condition the threshold is improved slightly, 25 $MN/m^{3/2}$, even though the yield strength increases from 310 $MN/m^{3/2}$ to 1070 MN/m^2 with aging.[25] The data in Fig. 21 also show the times-to-failure in wet air are greater than in dry air. Stress corrosion

crack velocity measurements have also been made on the aged 4.5% Nb alloy in laboratory air and related environments.[45] The results of 10% R.H. air tests are shown in Fig. 22. The data show that three regions of crack propagation exist and the K_{ISCC} is 22 MN/m$^{3/2}$.

McLaughlin *et al.*[50] studied the effect of heat treatment on the cracking behavior of U–5% Nb in 8-ppm Cl^- solutions. The specimens were aged at temperatures from 200 to 600°C for times of 2, 8, and 24 hr. The most susceptible material was aged at 450°C independent of the time while the most resistant material was aged at 550°C and above. The improvement that resulted above 450°C corresponds to the formation of a two-phase structure, presumably $\alpha + \gamma_2$.

6% Nb. The stress corrosion cracking behavior of U–6% Nb has also been studied fairly extensively. Koger[49] conducted tests on smooth U–6% Nb specimens ranging from as-quenched material to material which was quenched and overaged (600°C for 10 hr). Tests conducted in 0.1 *M* NaCl (pH 4, -200 mV) at stresses well below yield showed the quenched specimens and specimens aged at 150 and 200°C for 2 hr and at 600°C for 10 hr did not fail in 17 hr, while specimens aged at 250°C for 3 hr, 300°C for 3 hr, and 400°C for 2 hr failed. Specimens loaded slightly above the yield stress in 50-ppm Cl^- (pH = 4 no potentiostatic control) also showed a similar behavior: the low-temperature and high-temperature aged specimens did not fail in 17 hr, while the specimens aged at 250–400°C failed in 10 min or less. Other tests conducted at the same stress level for all of the heat treatments showed that overaged material was significantly more resistant to cracking than quenched material.

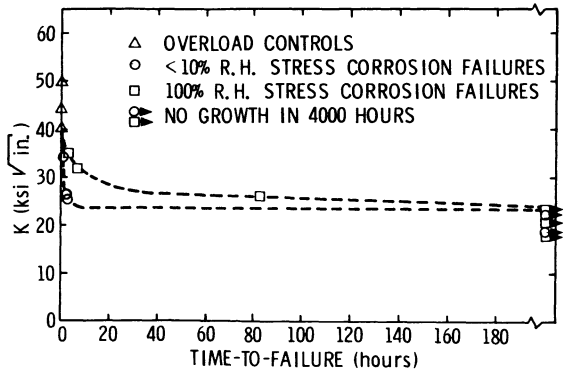

Fig. 21. The effect of the initial stress intensity and the time-to-failure for U–4.5% Nb aged at 260°C for 80 hr (after Magnani[25]).

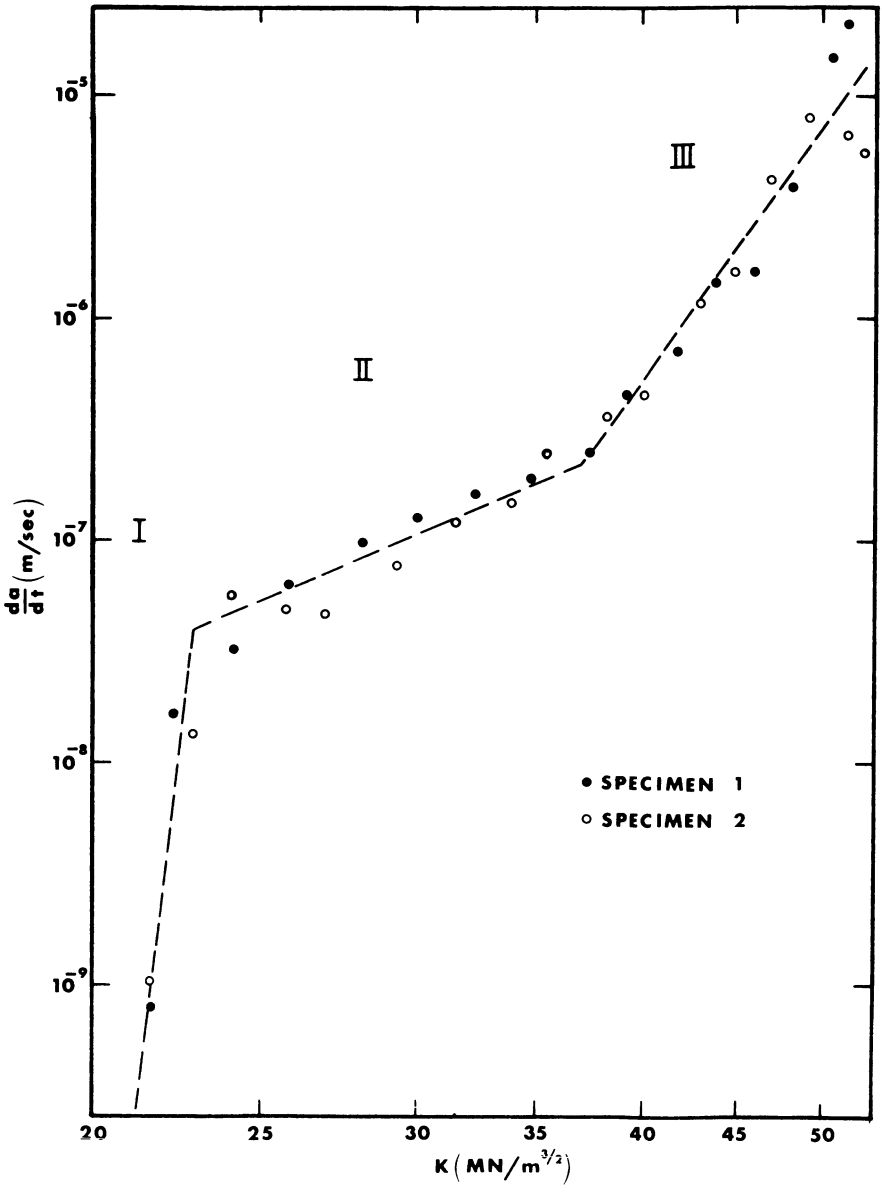

Fig. 22. The stress corrosion crack velocity of U–4.5 % Nb aged at 260 °C for 80 hr tested in 8 % R.H. air (after Magnani[45]).

Thresholds, K_{SCC} (not plane strain conditions), for quenched U–6% Nb have been determined in dry air, 100% R.H. air, and 50-ppm Cl^- environments.[43] The threshold in dry air is 38 $MN/m^{3/2}$, in wet air 22 $MN/m^{3/2}$, and in 50-ppm Cl^- 17 $MN/m^{3/2}$. These results show that water enhances cracking in O_2 environments even though it has been shown cracking does not occur in pure H_2O. Material aged at 200°C for 2 hr has thresholds 3 $MN/m^{3/2}$ lower than quenched material in 100% R.H. air and in 50-ppm Cl^-, 19 $MN/m^{3/2}$ and 13 $MN/m^{3/2}$ respectively.[43] Miller *et al.*[48] tested the 6-wt% alloy in 100% R.H. air in three underaged heat treatments, 250°C for 3 hr ($\sim$700-MN/m^2 yield), 254°C for 6.5 hr (810-MN/m^2 yield) and 360°C for 1.2 hr (1100-$MN/m^{3/2}$ yield). The thresholds were 22 $MN/m^{3/2}$ for the lower strength levels and only 11 $MN/m^{3/2}$ for the strongest material.

8.5% Nb. There is very little information available on the cracking behavior of U–8.5% Nb and no data on the effect of heat treatment. Unpublished data from this laboratory show K_{ISCC} is 19 $MN/m^{3/2}$ for quenched material in dry air and that propagation in humid air is slower than in dry air. Stephenson[51] reported that initiation in the $8\frac{1}{2}$-wt % alloy took longer than for the 4.5-wt % alloy.

Fracture Mode

Both intergranular and transgranular (refers to prior γ grain boundaries) stress corrosion cracking have been reported for U–Nb alloys. The 2.3% Nb alloy cracks transgranularly in both the underaged[47] α' and overaged $\alpha + \gamma_1$ conditions in air and in dilute Cl^- solutions. Figure 23 shows a stress corrosion fracture surface of quenched U–2.3% Nb which has been tested in wet air. This fractograph, which is also representative of a dry-air environment, shows heavy secondary cracking and evidence of the banded microstructure on the fracture surface. A fracture surface for the same material tested in a 50-ppm. Cl^- environment is shown in Fig. 24. The fracture surface indicates that cleavage has occurred and that the secondary cracking is crystallographic in nature.

Underaged specimens with higher Nb concentrations crack transgranularly or intergranularly depending on the environment. Transgranular (quasi-cleavage) cracking was observed for the U–4.5% Nb alloy in wet and dry air tests[25,42] and for dilute Cl^- solutions (<2, 5 ppm).[25] A mixed transgranular and intergranular cracking has been observed in more concentrated Cl^- solutions.[25,46] The U–6% alloy behaves in a similar manner. Quasi-cleavage cracking was observed in wet and dry air.[43] Figure 25 shows a wet-air fracture surface; note the heavy secondary cracking observed in this alloy

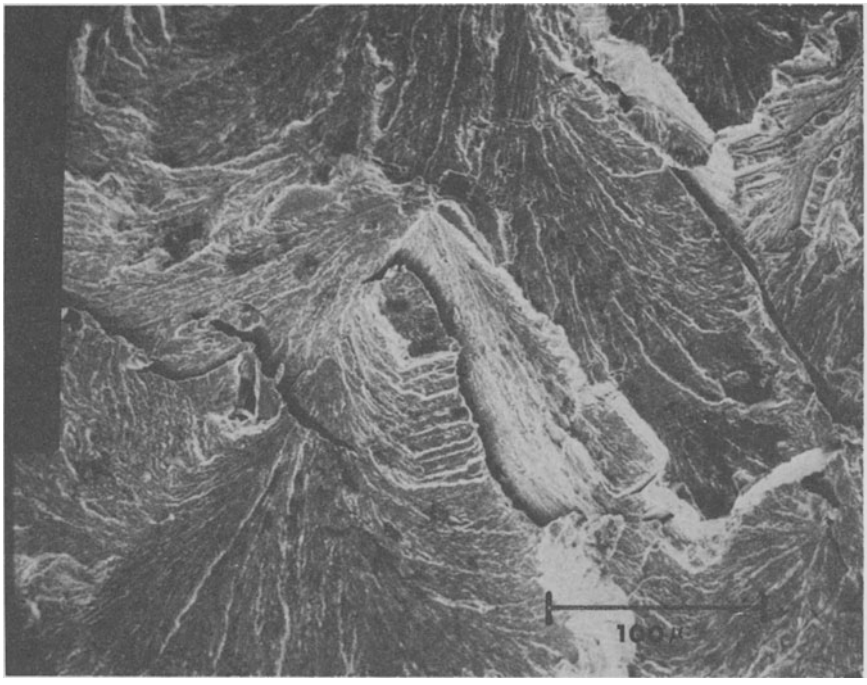

Fig. 23. Slow crack growth in quenched U–2.3% Nb tested in 100% R.H. air.

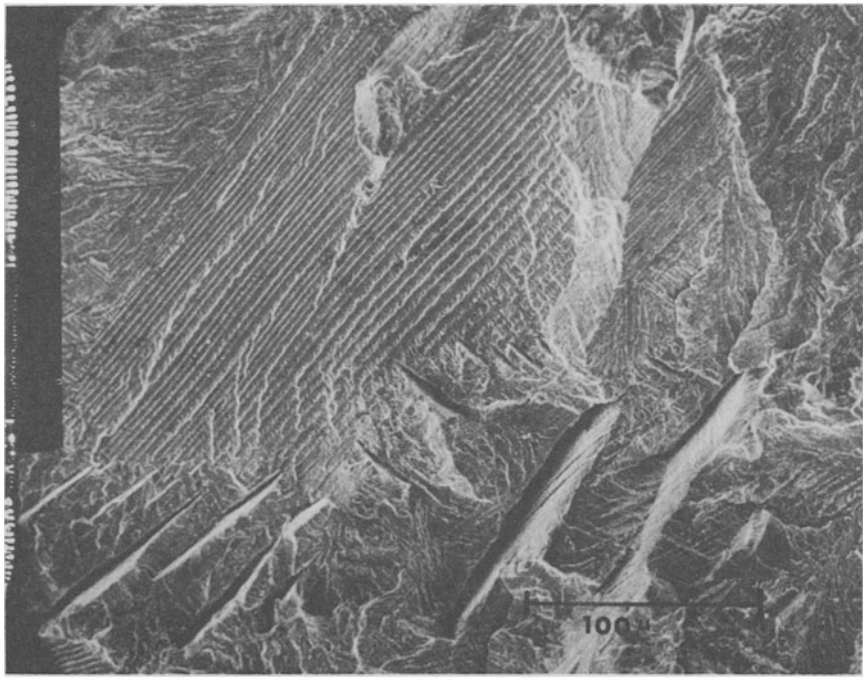

Fig. 24. Slow crack growth in quenched U–2.3% Nb tested in 50-ppm Cl^-.

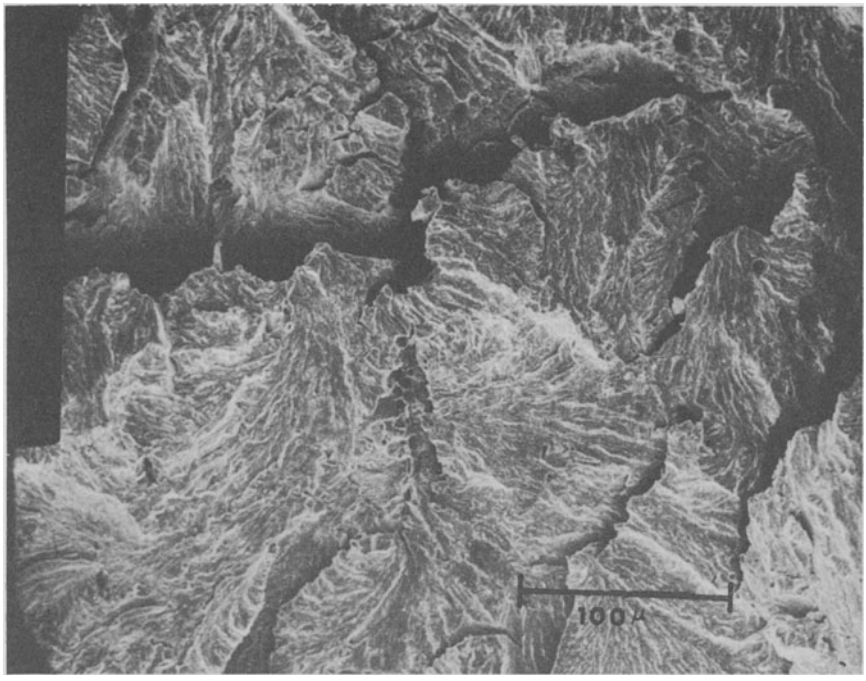

Fig. 25. Slow crack growth in quenched U–6% Nb tested in 100% R.H. air.

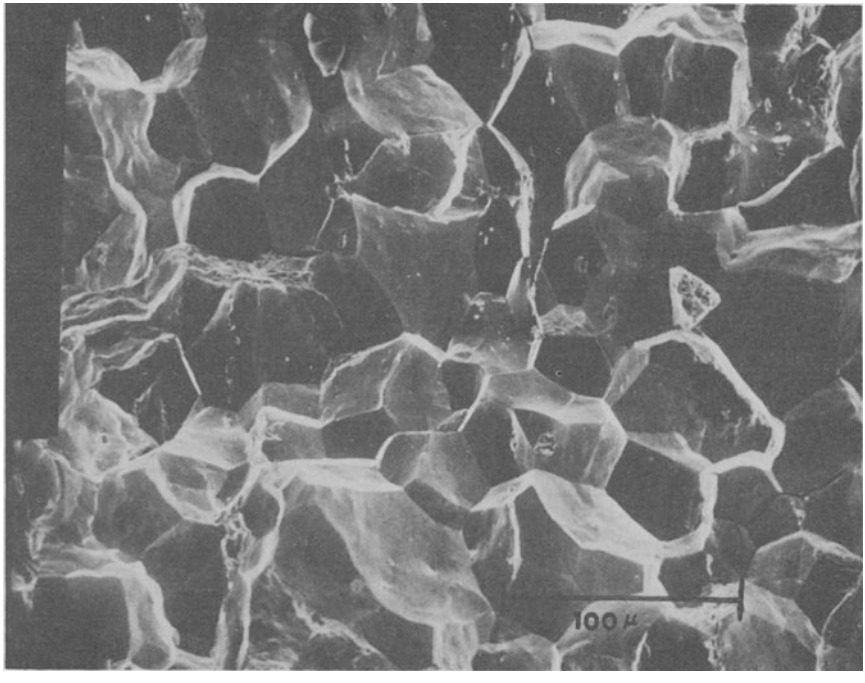

Fig. 26. Slow crack growth in quenched U–6% Nb tested in 50-ppm Cl^-.

when tested in wet air. In dilute Cl^- solutions the U–6% Nb alloy cracks with a mixed mode,[51] while in 50-ppm Cl^- intergranular cracking occurs[43] (Fig. 26). The 8.5% Nb alloy cracks intergranularly even in dilute Cl^-[51] and transgranularly in dry air. The fracture mode in overaged U–Nb alloys is not well-defined.[49]

These fractographic data show that the alloy composition, the environment, and the heat treatment all affect the stress corrosion fracture mode. Higher Nb concentrations and Cl^- favor intergranular cracking, while aging to the equilibrium structures favors transgranular cracking.

Summary

The U–Nb stress corrosion cracking data indicate that, as was the case with U–Mo alloys, O_2 will lead to stress corrosion cracking. Water vapor can also be detrimental to U–Nb alloys. The U–2.3% Nb alloy is embrittled by humidity in a manner similar to U and U–Ti alloys, while the 2.3 and 4.5% alloys will stress corrosion crack in water vapor. The U–6% Nb alloy will not crack in H_2O, but H_2O accelerates cracking in environments containing O_2.

The data have shown that overaged specimens are more resistant to stress corrosion cracking than underaged specimens. However, since a two-phase $\alpha + \gamma$ structure is formed on aging, the corrosion resistance will be lower. The stress corrosion fracture mode, transgranular, intergranular, or a mixed mode, is dependent on the environment and the alloy composition and heat treatment.

Uranium–Niobium–Zirconium Alloys

Part of the rationale for developing ternary U–Nb–Zr alloys is based on minimizing the internal stresses in metastable γ alloys. Both Mo and Nb have smaller atomic volumes than uranium and reduce the γ lattice parameter, while Zr has a larger atomic volume and expands the γ lattice when added to uranium. Therefore, the addition of Zr to U-Nb alloys should reduce the internal stress and produce a more stable alloy.

The only U–Nb–Zr alloy which has been studied to any significant extent is U–7.5% Nb–2.5% Zr. This alloy in the quenched condition, is in either a bcc or bct variant of the γ uranium phase, with the structure depending on, as of yet not well understood, differences in the chemistry of the alloy.[52] The stress corrosion cracking behavior of the ternary alloy is similar to that of the more Nb-rich U–Nb alloys. However, unlike the U–8.5% Nb alloy,

U–7.5% Nb–2.5% Zr is not embrittled by internal H_2. Tests have been conducted on specimens with H_2 concentrations up to 70 ppm (1.7 at. %) with no embrittlement observed.[8]

Some differences in the cracking behavior of smooth and precracked specimens have been observed in the U–Nb–Zr alloy and are attributed to the type of cracking occurring, transgranular oxide stress rupture or intergranular anodic dissolution.

Environment

As was the case with U–Mo and U–Nb alloys, O_2 has been identified as the principal stress corrodent for U–7.5% Nb–2.5% Zr in laboratory air and is required for both types of cracking observed in this alloy. Whitlow[40] showed that high relative humidities enhanced crack initiation in the air. Smooth specimens exposed to 92% R.H. air at 690 MN/m^2 failed in 0.3 hr, while specimens similarly stressed but exposed to 55% R.H. air did not fail in 200 hr. Weirick and Schoenfelder[53] conducted tests on smooth bend specimens to determine the environmental requirements for stress corrosion cracking in the ternary alloy. They stressed specimens at the yield strength in aqueous Cl^- solutions without O_2 and observed no failures in 5 months. However, once air was admitted to the chamber, failure occurred in 4 min. Similar tests conducted without the Cl^- did not exhibit failures in 960 days, showing that Cl^- is also required for cracking in smooth specimens. It is interesting to note that corrosion was not very great in the O_2-free Cl^- environment, but specimens exposed to the aerated Cl^- solutions corroded rapidly.

The results of tests conducted on precracked specimens in several environments are shown in Table 9. The data show that cracking will occur in O_2 and H_2 and that H_2O accelerates cracking but will not cause cracking by itself.[25] Tests conducted in various partial pressures of O_2 show that the O_2 threshold for cracking is less than 0.01 atm.[54] Stress intensity thresholds have not been determined in pure gases. However, the results of tests conducted in ~10% R.H. air, shown in Fig. 27, indicate K_{ISCC} is 20 MN/m$^{3/2}$ in this environment. In 100% R.H. air the times-to-failure are longer, but K_{ISCC} is about the same.[54]

The effect of relative humidity on cracking in environments containing O_2 is not straightforward. Miller[55] studied the effect of relative humidity from 0 to 100% on precracked specimens and found that specimens exposed to 20–90% R.H. had much longer failure times than specimens tested at either higher or lower relative humidities. The specimens in the intermediate

Table 9. Gaseous Environment Tests on U–7.5 wt% Nb–2.5 wt%Zr[a] $K \approx 33$ MN/m$^{3/2}$

Atmosphere	Time in Test, hr	Stress corrosion crack growth,[b] in.
Vacuum	4000	None
N_2 (dry)	4000	None
N_2 (water saturated)	1000	None
O_2 (dry)	3000	≃.040
O_2 (water saturated)	300 (failed)	≃.100
H_2 (dry)	10 (failed)	≃.100

[a] After Magnani, Ref. 25, material quenched and aged 150°C/hr.
[b] Average for a minimum of three specimens.

conditions often exceeded one year in test while specimens at either extreme failed in 20–100 hr.

The effect of Cl^- concentration on stress corrosion crack propagation has also been investigated.[46] The results for tests conducted in several Cl^- solutions are shown in Fig. 28. The data show that K_{ISCC} is lowered and the time-to-failure is decreased by increasing the Cl^- concentration. These results are summarized in Table 10. The thresholds are based on 1000-hr tests. Specimens exposed to 500-ppm Cl^- for very long times crack in the absence of an applied stress. This cracking is attributed in part to corrosion product wedging.[46]

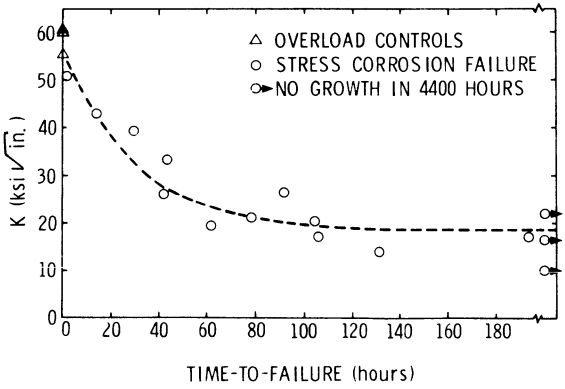

Fig. 27. The effect of the initial stress intensity and time-to-failure for U–7.5% Nb–2.5% Zr aged at 150°C for 1 hr tested in 10% R.H. air, (after Magnani[25]).

Table 10. The Effect of Cl^- Concentration on the Time-to-Failure and K_{ISCC} for U–7.5% Nb–2.5% Zr[a]

Solution, ppm Cl^-	Time-to-failure at 33 $MN/m^{3/2}$, hr	K_{ISCC}, $MN/m^{3/2}$
<2	10	17
5	0.4	11
25	0.2	11
50	0.2	5
500	0.03 – 0.1	5

[a] After Magnani, Refs. 25 and 46, material γ quenched and aged at 150°C for 1 hr.

Several investigators have reported that the cracking observed in Cl^- solutions will not occur in strong basic solutions[51,56,57] (pH > 12.5) and that NO_3 inhibits cracking.[56,57] The same studies report that anodic potentials accelerate crack initiation and that cathodic potentials inhibit initiation.[51,56,57]

Heat Treatments

Most of the experimental work on the U–7.5% Nb–2.5% Zr alloy has been conducted on as-quenched material and quenched material with a low temperature age (150°C for 1 hr). However, once the magnitude of the stress corrosion cracking problem in these conditions was realized several programs were initiated to determine the cracking behavior of materials in other heat treated conditions. Weirick[58] studied materials with a series of heat treatments that provided all of the basic microstructures observed in this alloy. The treatments he selected and their corresponding microstructures are (1) 150°C for 1 hr, γ_s; (2) 350°C for 24 hr, monoclinic α''; (3) 450°C for 9 hr, fine α precipitate in the prior γ grain boundaries; (4) 550°C for 9 hr, α precipitates in the grain boundaries and some decomposition of the matrix material to a lamellar α + Nb and Zr-rich γ; (5) 600°C for 8 hr, 40% of the γ decomposed to the lamellar α + Nb and Zr-rich γ. The results of the stress cracking tests are shown in Fig. 29. Crack initiation in the bend specimens was detected with acoustic emission equipment. The data in the figure show that the 600°C/8 hr material is the most resistant to initiation while the 350°C/24 hr material is the most susceptible. Weirick's tests also showed that propagation is the fastest in the most brittle material, 450°C/9 hr and the slowest in the 150°C/1 hr material.

Vaughn and Phalen[52] and Whitlow[40] tested the ternary alloy in the as-quenched condition; quenched and aged at 350°C for 4 hr; and quenched and aged at 600°C for 4 hr,[56] and 1 hr.[40] Both investigations found that the 600°C material is the least susceptible and that the 350°C material is the most susceptible.

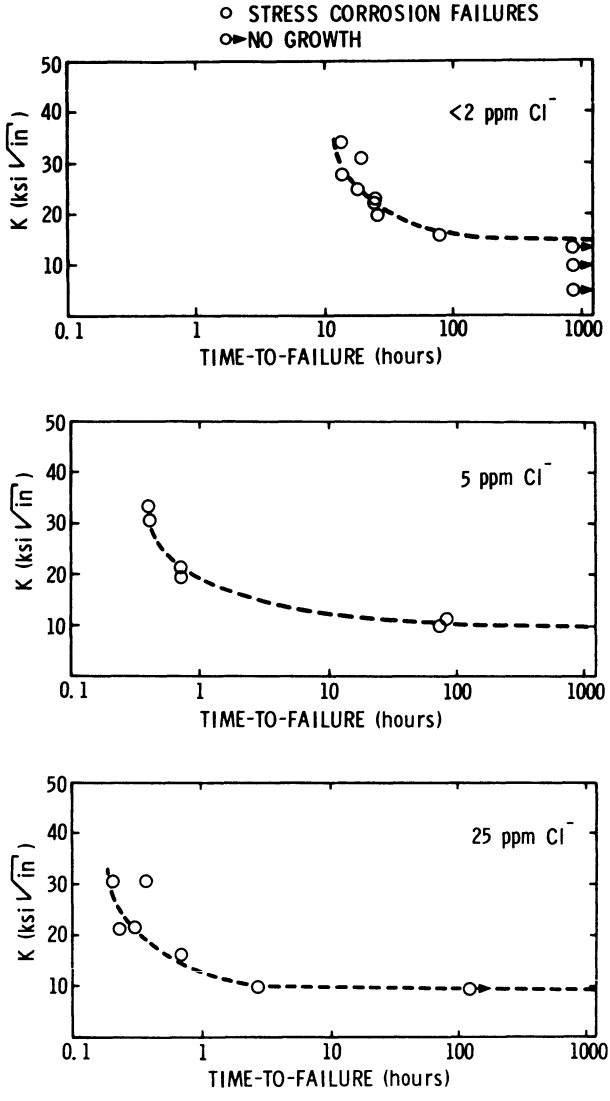

Fig. 28. The effect of Cl^- concentration on time-to-failure for U–7.5 % Nb–2.5 % Zr aged at 150 °C for 1 hr (after Magnani[25]).

Fractography

The importance of fractography in understanding the stress corrosion cracking of uranium alloys is well illustrated in U–7.5% Nb–2.5% Zr. If one assumes the intergranular and transgranular cracking observed in this alloy are caused by different mechanisms and that the transgranular mode, which has been observed only in precracked specimens, does not initiate easily, the discrepancies in the literature as to the environments required for cracking can be resolved. Intergranular stress corrosion cracking occurs in Cl^- solutions[25,46,51,57,58] and in humid air[25,54,55,59] in both smooth[51,57–59] and precracked[25,46,54,55] specimens. In the more concentrated Cl^- solutions, the intergranular cracking was mixed with transgranular dimple rupture,[25] indicating rapid crack propagation. In 100% R.H. air, another mixed mode was observed, intergranular cracking and quasi-cleavage, Fig. 30. The intergranular mode is reported to require H_2O, O_2, and Cl^- for initiation,[58] but only O_2 and H_2O for propagation.[54]

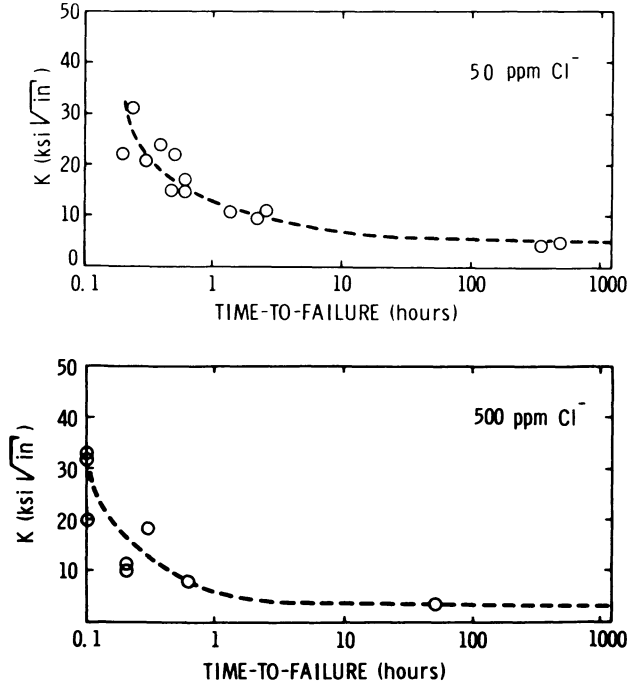

Fig. 28 (continued).

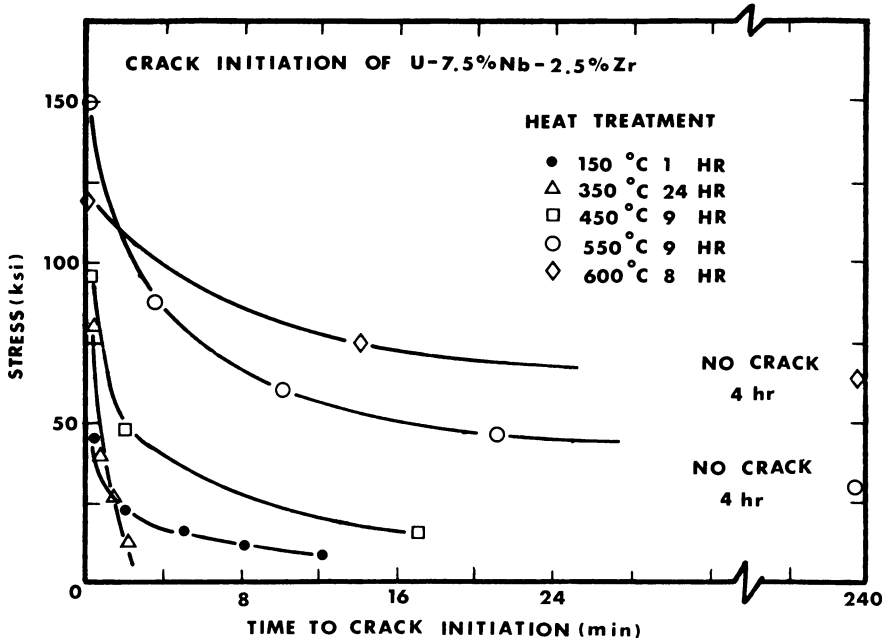

Fig. 29. The effect of heat treatment on the time to crack initiation in U–7.5% Nb–2.5% Zr in 10^{-3} MKCl with an applied potential 500 mV anodic to the rest potential (after Weirick[58]).

Transgranular stress corrosion cracking, quasi-cleavage, has only been observed in precracked specimens tested in air.[25,54,60] Figure 31 shows the fracture surface of a specimen tested in 100% R.H. air. The crack extension is quasi-cleavage, but a side-initiated intergranular crack also contributed to the ultimate failure of the specimen. The transgranular stress corrosion cracking requires O_2 but not Cl^- or H_2O.[25] $KClO_4$, which is a strong oxidizer, also leads to transgranular cracking.[51] The effect of potential on the cracking mode also indicates that a fundamental difference between the mechanisms exists. Anodic potentials lead to intergranular cracking while cathodic potentials lead to transgranular cracking.[51]

Summary

The U–7.5% Nb–2.5% Zr alloy is not embrittled by internal hydrogen, but does stress corrosion crack in numerous environments. Two types of stress corrosion cracking are observed in the alloy, each with its own fracture mode. The intergranular cracking initiates easily but requires O_2, Cl^-, and H_2O to do so. The transgranular stress corrosion cracking does not initiate easily and can propagate in pure O_2 or in solutions containing strong oxidizers such as $KClO_4$. The effect of relative humidity on the time-to-failure of ternary specimens, short-time failures at low and high relative humidities, and long-time failures at intermediate humidities, indicates that

different mechanisms are operative at the relative humidity extremes. In the intermediate humidities neither mechanism is optimized and the failure times are very long.

Studies of the effect of heat treatment on stress corrosion cracking susceptibility have shown that overaging to produce α + Nb and Zr-rich γ results in the most stress-corrosion-resistant U–Nb–Zr alloys, while heat treating in an intermediate temperature range ($\sim$350°C) for relatively short times, 4–24 hr, produces the most susceptible alloys.

Polynary Alloys

A series of polynary alloys containing small quantities of all of the potent γ stabilizers, Nb, Mo, Zr, Ti, and in some cases V, have been developed. The alloys would be expected to have an α' or α'' banded microstructure in the quenched condition. However, the stress corrosion cracking studies have been conducted on as-extruded material instead of on quenched and aged materials as was the case with the binary and ternary uranium alloys. In the as-extruded condition some decomposition into the equilibrium phases has

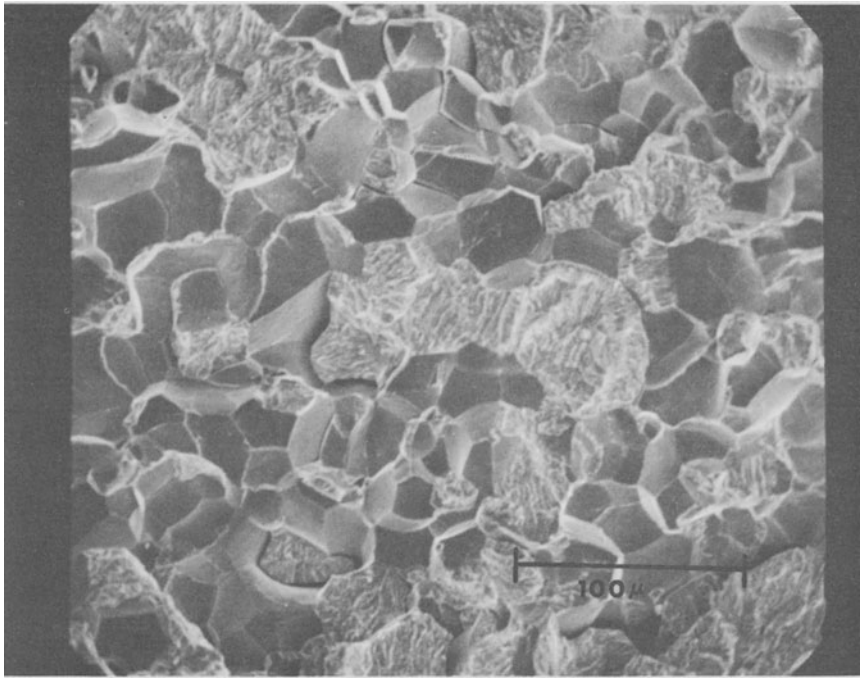

Fig. 30. Mixed intergranular and quasi-cleavage slow crack growth in 150°C/1 hr U–7.5% Nb–2.5% Zr tested in 100% R.H. air.

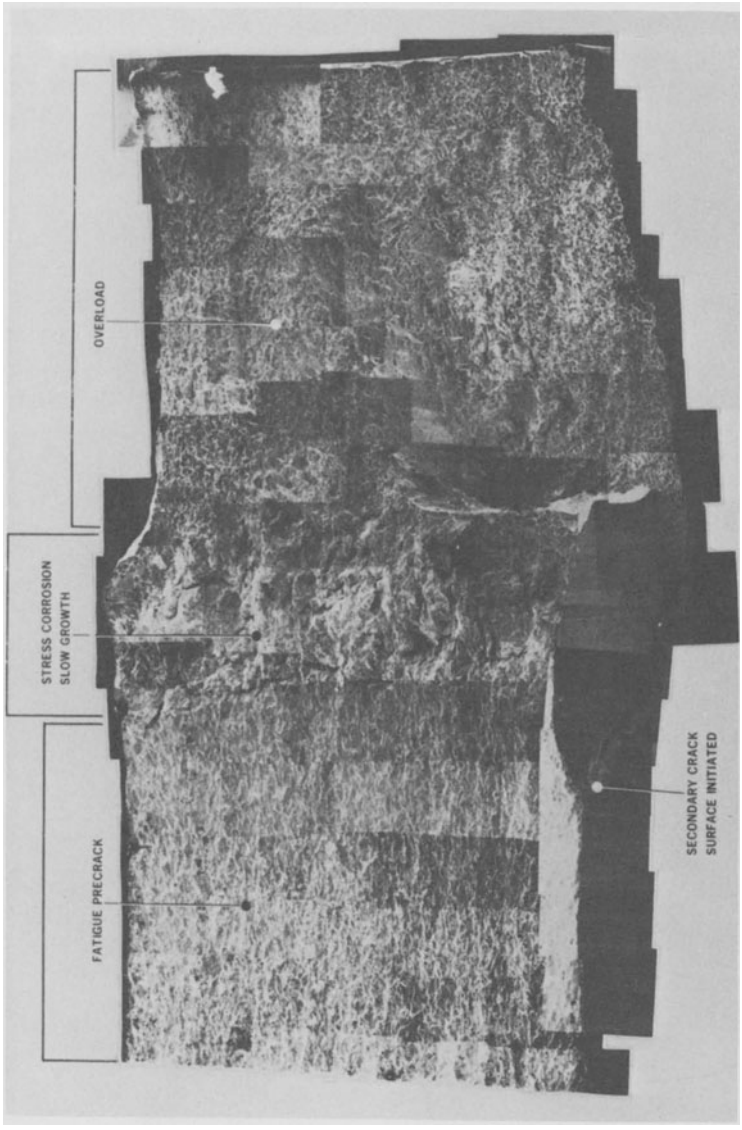

Fig. 31. A U–7.5% Nb–2.5% Zr stress corrosion fracture surface showing quasi-cleavage crack extension and side-initiated intergranular cracking. Specimen 0.5 cm thick.

Table 11. K_{ISCC} Values for As-Extruded Polynary Uranium Alloys

Alloy	Overload K, MN/m$^{3/2}$	K_{ISCC}, MN/m$^{3/2}$			
		100% R.H. air	H_2O (<1-ppm Cl^-)	50-ppm Cl^-	3.5% NaCl
U–½% Mo–½% Nb–½% Zr–½% Ti (½ Quad)	70	25	—	<20	—
U–¾% Mo–¾% Nb–¾% Zr–¼% Ti (¾ Quad)	51[a]	—	44[a]	—	13[a]
U–1% Mo–1% Nb–1% Zr–½% Ti (1 Quad)	35[a]	—	31[a]	10[a]	8[a]
U–1% Mo–1% Nb–1% Zr–½% Ti–½% V (1 Quint)	22[a], 24[b]	21[b]	16[a]	5[c], 7[b]	5[a]

[a] Reference 27.
[b] Reference 29.
[c] Reference 3.

taken place. These materials are subject to stress corrosion cracking, but there are no references as to the effect of the environment on ductility.

Environment

Table 11 shows the stress corrosion cracking thresholds obtained for the polynary alloys. The data show that as was the case with the binary alloy systems, the effect of H_2O on the cracking behavior is related to the reactivity of the alloy. The ½ Quad,* which is the most reactive alloy is susceptible to cracking in 100% R.H. air, while the ¾ Quad and 1 Quad are not even susceptible in immersion environments.[27] The Quint alloy, which is not very reactive, seems to behave in a contrary manner since it is susceptible to cracking in the immersion environment. However, the Quint alloy has a much higher yield strength than any of the other alloys,[27] and the enhanced susceptibility is attributed, at least in part, to this.

In Cl^- solutions all of the polynary alloys behave in a similar manner. First, the Cl^- concentration does not strongly affect the K_{ISCC} and second, while there is a large variation in thresholds among the various alloys, the degree of environmental degradation is approximately the same for all of them. K_{ISCC} is approximately 25% of the overload K. This shows that the toughness of the material plays a dominant role in the stress corrosion cracking process. This type of behavior was also observed in U–Ti alloys.

* See Table 11 for the chemical composition of the polynary alloys.

Fractography

The stress corrosion fracture mode in the as-extruded polynary alloys is transgranular.[27,29] A mixed quasi-cleavage and dimple rupture mode is observed in the H_2O environments, while pure quasi-cleavage is observed in the Cl^- environments except for the 1 Quint alloy in 3.5% NaCl. In the concentrated Cl^- environment the Quint alloy fails by cleavage.[27]

Summary

The polynary alloys have only been tested in the as-extruded condition in which there is some evidence of decomposition to the equilibrium phases. Despite this treatment, some of the alloys are susceptible to cracking in humid air or H_2O environments and all of the alloys are susceptible to cracking in Cl^- environments. The data also show that the effect of the Cl^- environments on all of the polynary alloys is the same when normalized with respect to the environment-free properties of the alloys.

EFFECT OF THE ENVIRONMENT ON EMBRITTLEMENT AND STRESS CORROSION CRACKING IN URANIUM AND URANIUM ALLOYS

Gases

Both uranium and uranium alloys are reactive with numerous gases including O_2, H_2O, and H_2. These are the gases which have been identified as either embrittling or cracking uranium and uranium alloys. Several reviews of the oxidation behavior of uranium and uranium alloys by O_2 and H_2O have been written, some of the more recent ones by Colmenares,[61] Orman,[19] and Cathcart.[62] At low temperatures uranium reacts with dry oxygen to form UO_{2+x}, while in pure H_2O uranium reacts more rapidly and forms UH_3 in addition to the dioxide. The addition of O_2 to H_2O reduces the reaction rate dramatically and reduces the amount of free H_2 generated by the $U + H_2O$ reaction. UO_{2+x} is still formed in the gas mixtures except under condensation conditions when a hydrated oxide, $UO_3 \cdot 0.8\ H_2O$, is formed.[19] Alloy additions reduce the reaction rate of uranium with O_2 and H_2O. The rate of H_2 generation from the reaction of a large number of uranium alloys with 100% R.H. O_2 at 75°C is shown in Fig. 32. The figure clearly shows that as the alloy content increases the reaction rate, and hence the H_2 liberation rate, decreases.

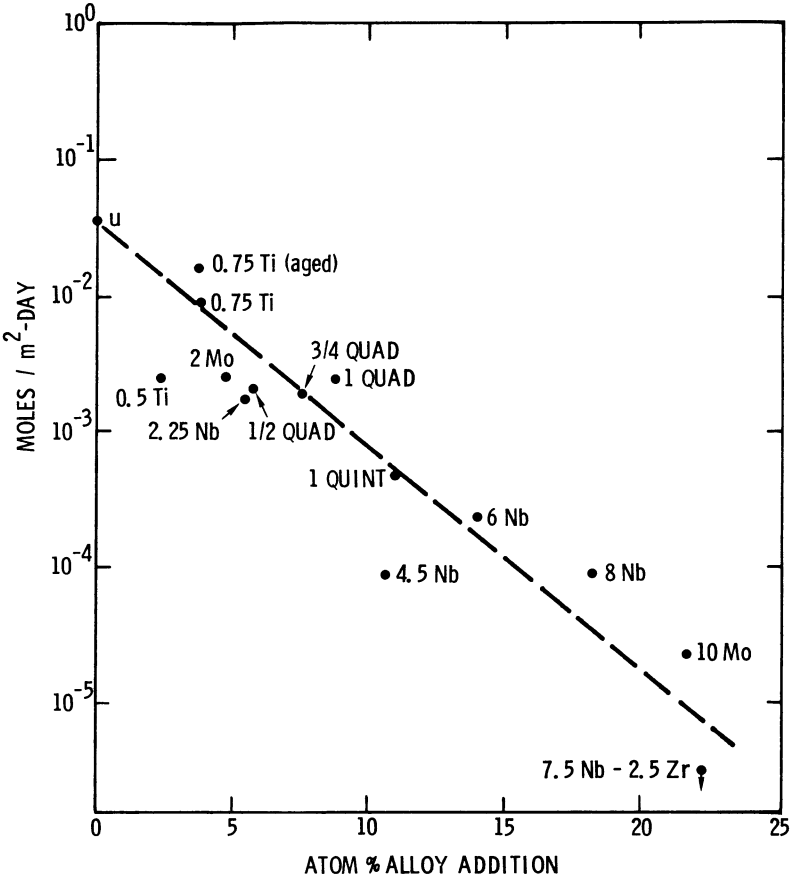

Fig. 32. The rate of H_2 generation of selected uranium alloys exposed to 100% R.H. O_2 at 75°C (the labeling is in wt %) (after Magnani[20]).

A recent review "Hydrogen in Uranium Alloys" by Powell and Condon[8] discusses the reactions of hydrogen with uranium and uranium alloys. The equilibrium partial pressure of H_2 above UH_3 is very low, $\ll 1$ Torr, at room temperature, and while the equilibrium pressure above the alloy hydrides has not been determined it should also be very low. Therefore, hydrides should be easily formed. In the presence of small quantities of O_2 the hydriding reaction is severely inhibited.

H_2O

Uranium and all of its alloys are degraded by water in the environment. Whitlow and Willows[16] and Adamson *et al.*[12] found that the ductility of

uranium is substantially lowered by humidity in the air. Under immersion conditions the ductility is lowered still further (see Fig. 6).[12] A similar type of behavior has been observed in U–0.75% Ti alloys by Jackson[21] and by Johnson *et al.*[22] Both investigations reported that for longitudinal extruded specimens the elongation is reduced from 20% in a vacuum to 2% in either 100% R.H. air[22] or in water immersion.[21] Zehr[41] observed that the 2.3% Nb alloy was also embrittled by humid air and H_2O immersion.

U–0.75% Ti[23] and U–4.5% Nb[45] stress corrosion crack in H_2O while U–6% Nb[43] and U–7.5% Nb–2.5% Zr[25] will not crack in pure H_2O. However, H_2O does affect the cracking behavior of all of the alloys, and the addition of water to O_2 environments dramatically enhances the susceptibility of the alloys to stress corrosion cracking. Only small additions of H_2O are required to enhance cracking. Studies on U–4.5% Nb,[45] and on the ternary alloy[55] have shown that the susceptibility will eventually decrease as the relative humidity is increased. For the ternary alloy, as saturation is reached, the stress corrosion fracture mode will change and the susceptibility will increase once again.[60] Figure 33 shows stress corrosion cracks in the ternary alloy formed in 96 and 100% R.H. air. The fracture mode is transgranular in the drier environment and predominantly intergranular in the saturated environment.

O_2

O_2 will cause stress corrosion cracking in all uranium alloys except U–0.75% Ti. In fact, O_2 inhibits the cracking of U–0.75% Ti in H_2 and H_2O, which is not surprising since this type of cracking is attributed to the formation of uranium hydride and O_2 inhibits the hydriding of uranium and uranium alloys. Weirick and Shoenfelder[53] and Macki and Kochen[44] showed that O_2 is required for crack initiation in U–7.5% Nb–2.5% Zr and U–4.5% Nb, respectively, while Pridgeon[31] and Peterson and Vandervoort[32] observed a similar behavior with U–Mo alloys. The author has shown that crack propagation will occur in U–4.5% Nb,[45] U–6% Nb,[43] and U–7.5% Nb–2.5% Zr[63] in O_2. While several uranium alloys crack in other environments, the investigations referred to above show that O_2 is the principal stress corrodent for uranium alloys in the air.

H_2

It has been reported that H_2 does not affect the ductility of uranium in dynamic tests[5] or the load carrying ability in static tests.[12] However, these results are probably due to oxides and/or impurities in the H_2. In the

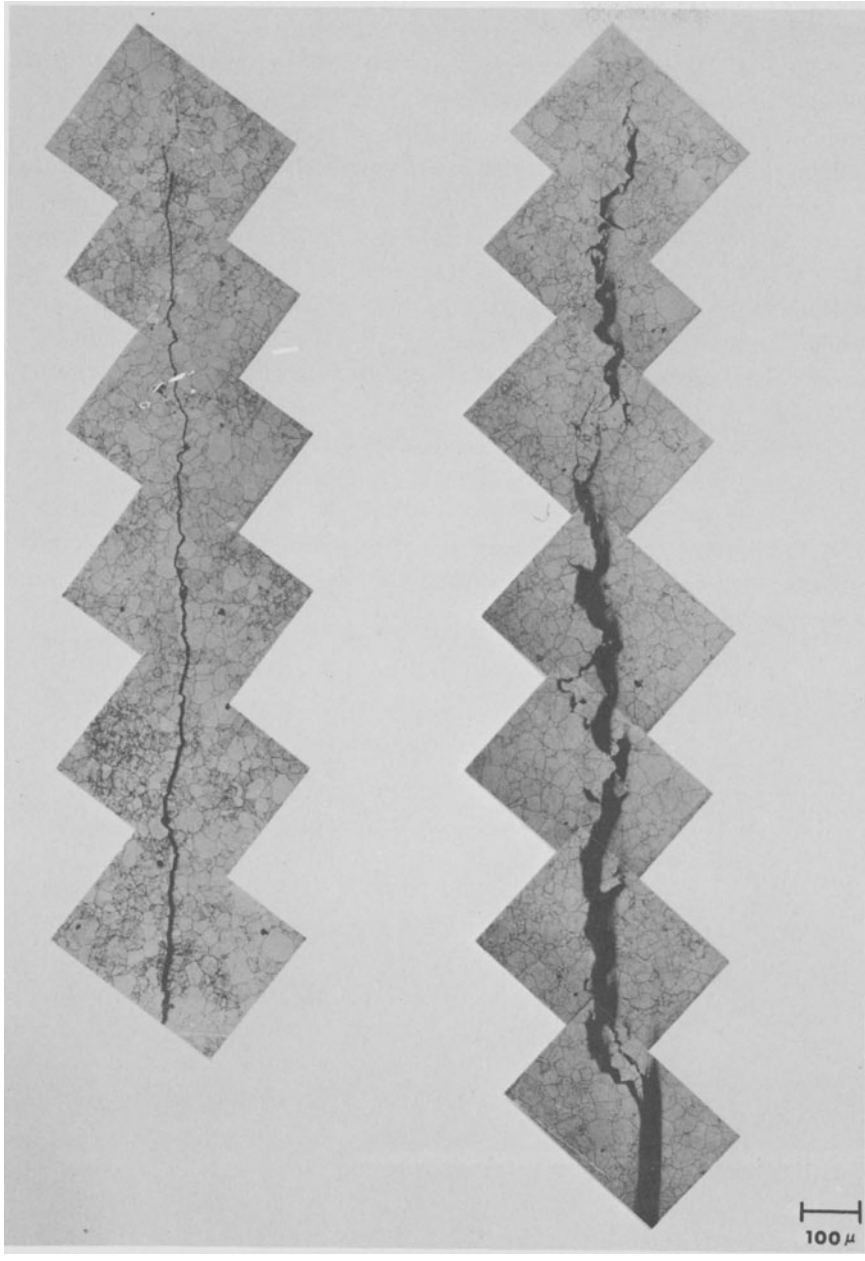

Fig. 33. U–7.5 % Nb–2.5 % Zr aged 1 hr at 150 °C stress corrosion cracks after 125 hr exposure to 96 % R.H. air (left) and 100 % R.H. air (right), $K = 38\ MN/m^{3/2}$ (after Chen[60]).

absence of an oxidized surface and O_2 or H_2O impurities in the gas, the H_2 and the metal should react to form UH_3, which would be expected to affect the properties to some extent. There is no information available concerning the effect of H_2 on the ductility of uranium alloys, but once again some effect is expected. Crack propagation in U–6% Nb,[43] U–7.5%–2.5% Zr,[25] and U–0.75% Ti[24] occurs in H_2 environments, and there is no reason to believe propagation will not occur in uranium and in all of the alloys in this environment.

The only alloy which has been studied in H_2 to any significant extent is U–0.75% Ti.[24] Recent crack velocity studies on this material have shown that cracking is proportional to $P_{H_2}^{\frac{1}{2}}$. The cracking is attributed to the wedging action of UH_3 at the crack tip (see Fig. 9); and once the hydride forms, crack propagation continues in the absence of an applied stress.

Electrolytes

Several stress corrosion cracking studies have been conducted in aqueous solutions. In this section the influence of several of the more important variables will be briefly reviewed.

Effect of Cl^-

Chloride ions dramatically affect the stress corrosion cracking behavior and the electrochemical behavior of uranium alloys. Passivity is destroyed and pitting is often induced. Levy *et al.*[64] found that small additions of Cl^- to H_2SO_4 solutions destroyed passivity and induced pitting in U, U–1.8% Mo, U–3.5% Mo, U–1.75% Ti, and U–3.5% Ti. Stephenson[51] observed a similar behavior in U–7.5% Nb–2.5% Zr. The aggressive nature of Cl^- is illustrated by studies of Bullock and Condon,[56] wherein they found that the rest potential of U–7.5% Nb–2.5% Zr is not affected by oxide coatings in Cl^- (Br^-) solutions to the extent it is in other electrolytes and that the density of potential contours increases in Cl^- (Br) solutions compared to other electrolytes. These data suggest that the Cl^- (Br) either penetrates the oxide or forms uranyl complexes with the oxide.[56]

Several investigations have shown that Cl^- is required for crack initiation in uranium alloys. Weirick and Schoenfelder[53] showed that stressed smooth U–7.5% Nb–2.5% Zr specimens survived 960 days in oxygenated water but failed in a matter of minutes when Cl^- was present. Macki and Kochen[44] observed a similar behavior for U–4.2% Nb; stressed

smooth specimens survived 10,000 hr in Cl^--free environments but failed in about 3 hr when 50-ppm Cl^- was present.

The magnitude of the effect of Cl^- on stress corrosion crack propagation in uranium alloys is inversely proportional to the reactivity of the alloy. The U–0.75% Ti alloy is the alloy least affected by Cl^-. It has been shown that: (1) K_{ISCC} is lower in Cl^- solutions than in H_2O, but the magnitude of the effect is not as great as in the more highly alloyed materials; and (2) the stress corrosion crack velocity is not dramatically affected by the Cl^- concentration.[23] Cl^- dramatically affects K_{ISCC} of the polynary alloys, but increasing the concentration from 50 ppm to 3.5% NaCl did not significantly affect the threshold. K_{ISCC} in Cl^- solutions is approximately 25% of the overload stress intensity for each of the alloys. The cracking thresholds in H_2O (< 1-ppm Cl^-) are between 50 and 85% of the overload stress intensities showing the Cl^- effect is quite large.

The cracking behavior of U–4.5% Nb, U–6% Nb, and U–7.5% Nb–2.5% Zr are also affected by Cl^-. The Cl^- concentration does not affect K_{ISCC} in the U–4.5% Nb alloy, but does affect the time-to-failure and presumably the crack velocity.[46] The time-to-failure and the threshold for the ternary alloys are affected by the Cl^- concentration. In 1000-hr tests K_{ISCC} decreases from 17 $MN/m^{3/2}$ in < 2-ppm Cl to 5 $MN/m^{3/2}$ in 500-ppm Cl^-, while the time-to-failure at 33 $MN/m^{3/2}$ decreases from 10 hr to about 4 min for the same environments.

Effect of pH

Hughes *et al.*[18] showed that uranium is embrittled in Cl^--free solutions only between pH 5 and 10. Johnson *et al.*[22] conducted similar tests on U–0.75% Ti and found the range of susceptibility is increased and that

Table 12. The Relationship between pH and Time-to-Failure for U–7.5% Nb–2.5% Zr in 8-ppm Cl^- Solutions[a]

pH	Time-to-failure
4	9 min
6	15 min
8.5	4 hr
12.5	No failure in 26 hr

[a] After Stephenson, Ref. 51, material quenched and aged at 150°C for 1 hr.

embrittlement occurs between pH values of 2 and 12 and hence only strong acids and bases can prevent embrittlement.

The pH also has an effect on the stress corrosion cracking susceptibility of U–7.5% Nb–2.5% Zr. The results of time-to-failure tests conducted in solutions with different pH values are shown in Table 12. The lack of stress corrosion cracking in basic solutions correlates with the passivity observed in 0.5-N and 1-N NaOH solutions with dilute Cl^- present.[51] Koger[57] also found that the ternary alloy is passivated in basic solutions but that passivity can be destroyed by high Cl^- concentrations.

Effect of Potential

Brettle and Orman[65] found that both the ultimate tensile strength and the ductility of uranium in Cl^- solutions are affected by the applied potential. The relationship between elongation and potential is shown in Fig. 34. The figure shows that the elongation decreases from almost 30% to about 10% as the potential is made more cathodic than -1250 mV (SCE). Hydrogen is generated at these potentials and the reduction of ductility is presumably caused by hydrogen embrittlement. At potentials more anodic than -1200 mV (SCE) the ductility is even lower, $<5\%$ elongation. The embrittlement at these potentials is attributed to stress corrosion cracking.[65]

The applied potential also affects the cracking behavior of uranium alloys. Stephenson[51] found that anodic potentials enhanced crack initiation in U–7.5% Nb–2.5% Zr and cathodic potentials inhibited crack initiation. The cracking under anodic potential control is intergranular, while the cracking under cathodic potential control is transgranular. Bullock and Condon[56] found that cracking initiated under anodic conditions could be stopped by applying cathodic potentials which led them to believe the mechanism of cracking for this alloy does not deal with H_2 embrittlement. Anodic potentials also enhance cracking in the U–6% Nb alloy.[49]

Inhibitors

Several inhibitors have been found for corrosion and stress corrosion cracking in uranium alloys. Levy *et al.*[64] found NO_3^-, CrO_4^-, and SO_4^{-2} inhibited the dissolution of U–1.8% Mo, U–3.75% Mo, U–1.75% Ti, and U–3.4% Ti, with CrO_4^- being the most effective. Stephenson[51] found that ClO_4^- stopped the intergranular cracking in U–7.5% Nb–2.5% Zr and that the specimens failed by quasi-cleavage cracking in this environment. Bullock and Condon[56] found evidence of passivation in 1 *N* KNO_3–0.01 *N* KCl solutions and that stress corrosion cracking is inhibited by the NO_3^-. They

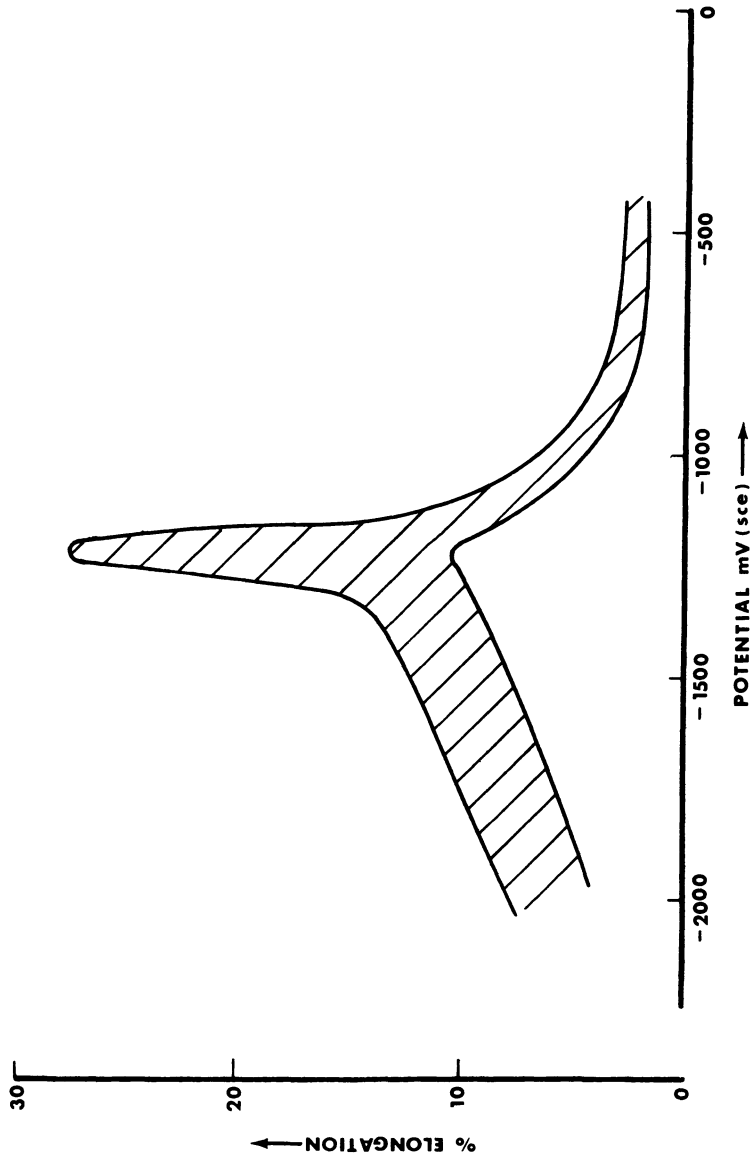

Fig. 34. The relationship between potential and elongation for uranium in 0.17-M NaCl (after Brettle and Orman[65]).

also found CN^- acted as a cracking inhibitor. The inhibiting effects of NO_3^- on stress corrosion cracking of uranium alloys was also observed by Koger.[57]

Effect of Temperature

Almost all uranium alloy stress corrosion cracking studies have been conducted at room temperature, and in only a few cases has the effect of temperature on cracking been determined. Pridgeon[31] found that the susceptibility of the U–5% Mo alloy to cracking in laboratory air increased with temperature above room temperature and that cracking did not occur below 10°C. His data yielded an activation energy of 6.3 Kcal/mole for the temperature range 25–100°C. The effect of temperature on the stress corrosion crack velocity of U–4.5% Nb alloy in 10% R.H. air has also been investigated.[45] The crack velocities as a function of K at several temperatures are shown in Fig. 35. The data show that the temperature affects the velocity in region II (intermediate K), and that in region III (highest K region) the effect of temperature disappears as K approaches K_{IC} ($\sim 55\ MN/m^{3/2}$). Within experimental error neither K_{ISCC} nor the velocity are affected by temperature in region I (lowest K). The activation energy for the region II data above room temperature is 7 Kcal/mole. The activation energy increases as the temperature decreases below room temperature, with a value of ~ 40 Kcal/mole obtained at the lowest temperature tested, 3°C.

Temperature tests on U–0.75% Ti in H_2 have shown that the activation energy above room temperature is approximately 8 Kcal/mole for region II cracking.

THE EFFECTS OF METALLURGICAL PARAMETERS ON EMBRITTLEMENT AND STRESS CORROSION CRACKING

Heat Treatment

The potent γ stabilizers of U (Mo, Nb, Zr, and Ti) are very soluble in the high-temperature γ phase and almost insoluble in the room temperature α phase of uranium. Therefore high-temperature aging of quenched uranium alloys leads to the formation of an equilibrium two-phase alloy, $\alpha + \gamma$ (a solute-rich phase). Slow cooling the alloys instead of quenching from the γ phase field often leads to the same basic two-phase structure. Since one of the purposes of alloying uranium was to prevent the formation of the anisotropic α phase, almost all uranium alloys are quenched to retain the γ phase or to

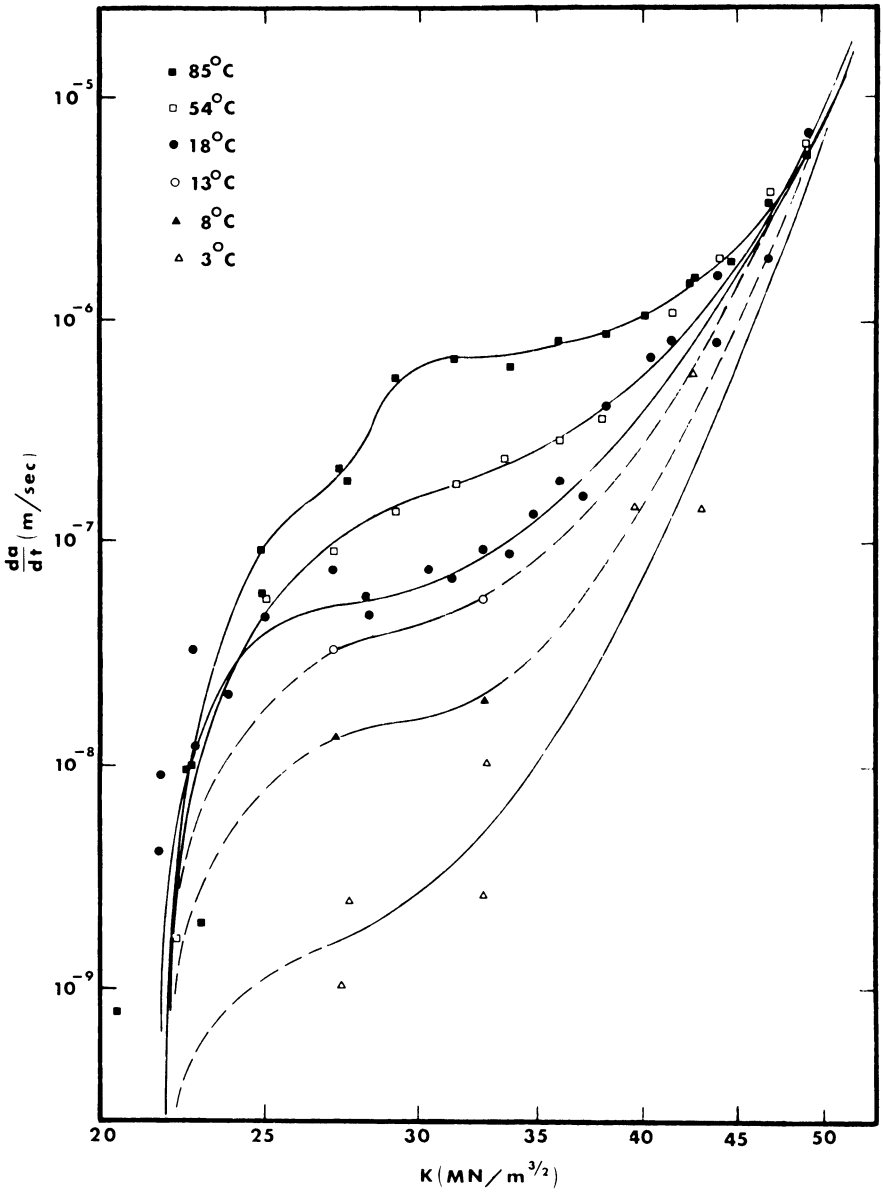

Fig. 35. The effect of temperature on the stress corrosion crack velocity of U–4.5% Nb (260 °C/80 hr) in 10% R.H. air (after Magnani[45]).

form a metastable variant of the α phase (α′ or α″), depending on the amount of alloy addition present (see Table 1). The alloys are then aged to improve the mechanical properties when required.

The data for all of the alloy systems show that the susceptibility of the quenched material to stress corrosion cracking increases with aging until the equilibrium two-phase structure starts to form. The susceptibility to cracking then decreases with continued aging. The equilibrium two-phase structure is the structure most resistant to stress corrosion cracking. A more detailed discussion of the effect of heat treatment on cracking susceptibility of alloys in the major uranium alloy systems can be found in the sections on the individual alloys.

Cold Work

The effect of cold work on the stress corrosion cracking susceptibility of uranium alloys has only been reported for U–7.5% Nb–2.5% Zr.[51,54,56,57] The data show that stress corrosion cracking in worked materials is always transgranular and that the most significant improvements in performance because of cold work occurs in environments which would normally lead to intergranular cracking. Stephenson[51] tested specimens which had crack propagation perpendicular and parallel to the direction of rolling and found that even specimens which had propagation parallel to the rolling direction had an increased resistance to stress corrosion cracking. As would be expected, the specimens with propagation across the elongated grains (propagation perpendicular to the rolling direction) were even more resistant to cracking.

In environments which lead to transgranular cracking, such as laboratory air, cold-worked specimens with cracking perpendicular to the rolling direction have approximately the same K_{ISCC} as nonworked specimens.[54] The data for the cold-worked specimens are shown in Fig. 36. The overload stress intensity for the worked material is much lower than for the nonworked material, 36 $MN/m^{3/2}$ versus 60 $MN/m^{3/2}$. Therefore, even though the cracking thresholds are the same for the worked and nonworked material, the extent of the environmental degradation is not as great in the worked material.

Surface Condition

Stephenson[51] tested the U–7.5% Nb–2.5% Zr alloy with an abraded surface, with a machined surface, and with a surface produced by a 75°C treatment for 60 hr. The results of his stress corrosion cracking tests show

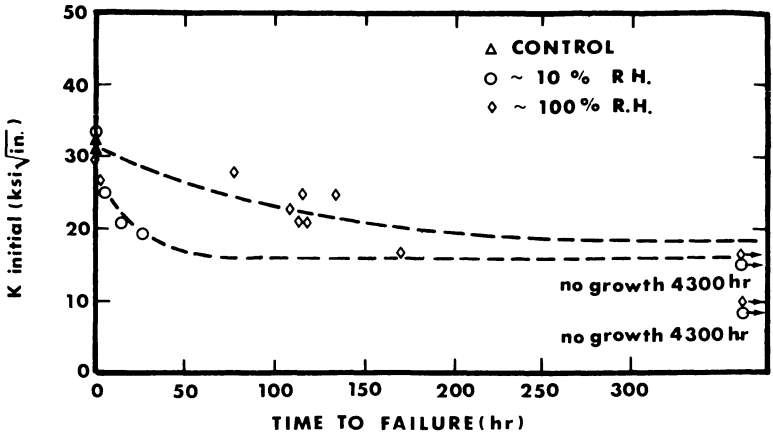

Fig. 36. The relationship between initial stress intensity for U–7.5% Nb–2.5% Zr 50% cold reduced (after Magnani, Romero, and Miglionico[54]).

that surface oxides not only increase the susceptibility to cracking but also make the rest potential more anodic, see Table 13. As-quenched surfaces are heavily oxidized and also increase the susceptibility of the ternary alloy to cracking.[59] However, U–7.5% Mo behaves the same with an as-quenched surface or with a machined surface.[34] Electropolishing improves the performance of the ternary alloy[57] (in very corrosive environments the electropolished specimens are more susceptible than machined specimens), but had no effect on the ductility of U–0.75% Ti.[21]

The data indicate that oxides on uranium alloy surfaces are detrimental to the alloy when the stress corrosion cracking is caused by an anodic dissolution mechanism. When cracking is not due to dissolution, as is the case with U–7.5% Mo and U–0.75% Ti, one would not expect the surface condition to influence the behavior of the alloy as dramatically.

Table 13. The Effect of Surface Condition on Stress Corrosion Cracking in U–7.5% Nb–2.5% Zr[a]

Surface condition	Rest Potential, SHE[b]	Time to crack initiative	Time to failure
Oxide coated (75°C/60 hr)	+106 MV	80 min	115 min
Machined (+room temp oxide)	+ 88 MV	21 hr	22 hr
Abraded	− 3 MV	79 hr	80 hr

[a] After Stephenson, Ref. 51, material aged at 150°C for 1 hr.

[b] Standard hydrogen electrodes.

Grain Size

The effect of grain size on stress corrosion cracking in uranium alloys has only been determined for U–5% Mo.[31] The data, shown in Fig. 37, indicate the threshold for the transgranular stress corrosion cracking decreases as the grain size increases. A Stroh-Petch relationship is obeyed wherein fracture threshold is proportional to the grain diameter to the half-power.

Specimen Orientation

Uranium and uranium alloy mechanical test and stress corrosion cracking specimens have been fabricated out of round rolled plate and extrusions, with the vast majority out of plate. Metallographic examination of the materials has not shown orientation effects for either type of material. The specimens fabricated out of plate have also not shown any evidences of a relationship between specimen orientation and embrittlement and stress corrosion cracking.

Specimens fabricated out of extruded stock have shown some evidence, though minor, of an orientational effect on embrittlement and stress corrosion

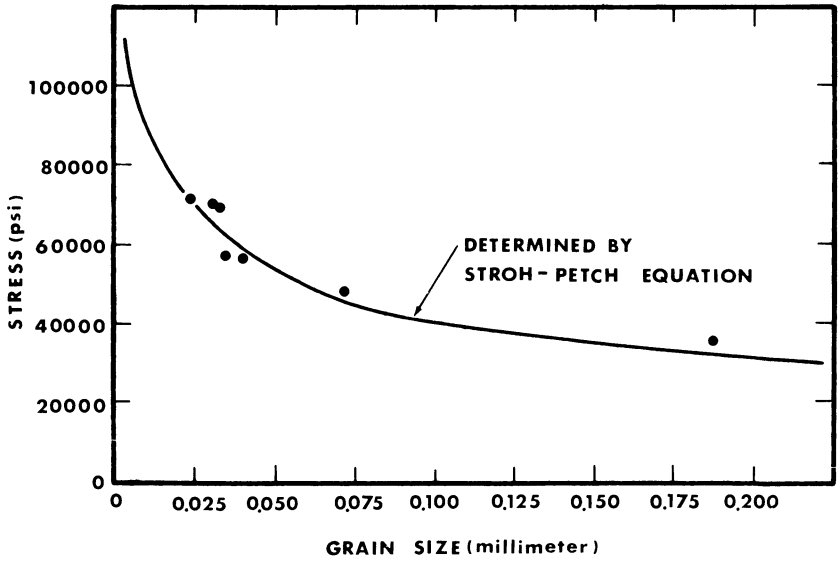

Fig. 37. The relationship between stress corrosion cracking threshold and grain size for quenched U–5% Mo in laboratory air (after Pridgeon[31]).

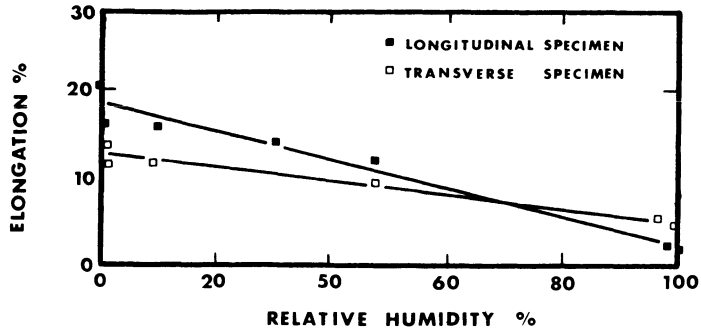

Fig. 38. The effect of the relative humidity on ductility in U–0.75 % Ti aged at 350 °C for 24 hr (after Jackson[21]).

cracking. It should be pointed out that the wall thicknesses of the uranium alloy extrusions were too thin to allow for the fabrication of specimens with radial fracture planes. Jackson[21] has studied the effect on orientation on the ductility of U–0.75 % Ti. The results of his tests are shown in Fig. 38. The data show that transverse specimens have a lower ductility than longitudinal specimens in a vacuum and a higher ductility in high relative humidities. Therefore, the influence of the environment on ductility is more pronounced

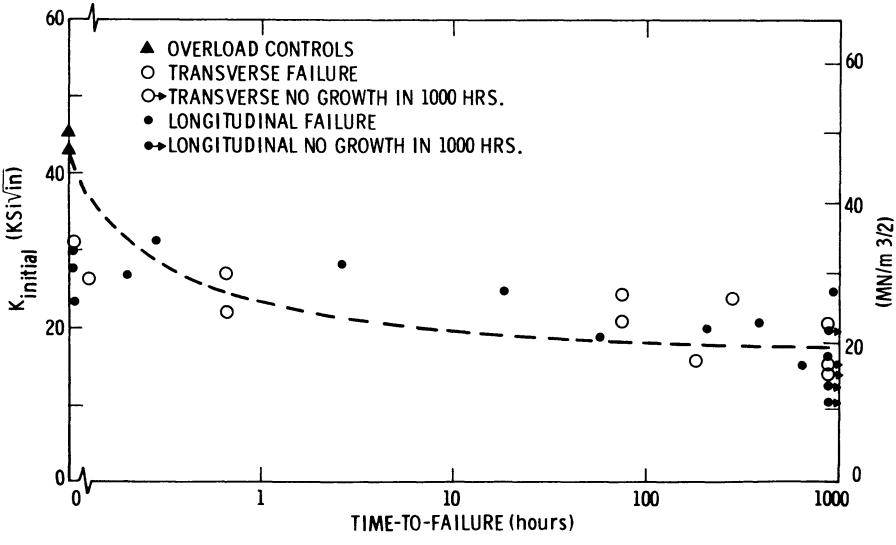

Fig. 39. The effect of initial stress intensity on the time-to-failure for extruded U–0.75 % Ti aged at 380 °C for 6 hr tested in 50-ppm Cl^- (after Magnani[23]).

in the longitudinal specimens. The effect of orientation on K_{ISCC} for U–0.75% Ti has also been determined.[23] Longitudinal specimens with cracking in the radial and transverse direction and transverse specimens with cracking in the radial and longitudinal direction were evaluated. The data show there is no effect from either the direction of propagation or the propagation plane on stress corrosion cracking. The results of tests in 50-ppm Cl^- are shown in Fig. 39. The data are grouped according to the cracking plane to illustrate this has no effect on the cracking behavior. Similar results showing a lack of an orientation effect were obtained in a 100% R.H. air environment.

Crack propagation studies on several orientations of extruded U–4.5% Nb have been conducted at this laboratory. The results of tests in 50-ppm Cl^- indicate that transverse specimens are slightly more susceptible to stress corrosion cracking than longitudinal specimens, $K_{ISCC} \simeq 15\ MN/m^{3/2}$ compared to $18\ MN/m^{3/2}$. The data also show that cracking direction does not affect the stress corrosion cracking behavior of this material.

Impurities

Certainly the impurity that most dramatically affects the properties of uranium and uranium alloys is hydrogen. It has been shown that very small quantities of hydrogen (< 1 ppm) in uranium reduce the ductility,[8,12] and Powell and Condon[8] have shown that similar effects occur in several uranium alloys. They found the amount of H_2 required to embrittle the alloys was significantly greater than the amount required for U; U–0.75% Ti is embrittled by about 3 ppm, U–8.5% Nb requires about 15 ppm, and U–7.5% Nb–2.5% Zr is not embrittled by 70 ppm of H_2.

Another impurity that is reported to affect the properties of uranium alloys in an environment is carbon. Both Peterson and Vandervoort[32] and Beaubron[66] have studied the effect of carbon level on the cracking threshold of smooth specimens of U–10 wt% Mo in laboratory air. They found that as the carbon level increases the threshold decreases. These data and data from U–Mo–Ti alloys are shown in Table 14. The U–Mo–Ti alloys are included since the primary objective of the addition of Ti to U–Mo was to reduce the carbon content of the alloy by forming TiC, which can be removed from the melt. The addition of Ti did have a beneficial effect on the thresholds presumably due to the lowering of the carbon content.

The effect of other impurities on the cracking behavior of uranium or uranium alloys has not been studied systematically.

Table 14. The Effect of Carbon Content on the Threshold for Stress Corrosion Cracking in U–Mo and U–Mo–Ti Alloys

Alloy	C, ppm	Threshold, MN/m^2	Reference
U–10% Mo	1000	310	40
„	408	258	32
„	190	434	66
„	90	497	66
„	85	497	32
U–8% Mo–0.5% Ti	75	431	37
U–10% Mo	70	518	32
„	65	604	32
U–8% Mo–1% Ti	15	745	32

MECHANISMS

Three basic types of mechanisms have been proposed for the embrittlement and stress corrosion cracking of uranium and uranium alloys. A hydride formation mechanism is proposed to be responsible for the embrittlement and cracking of uranium and the reactive alloys, which are the ones with low levels of alloy addition. The intergranular cracking observed in the alloys with the higher levels of alloy additions is attributed to an anodic dissolution mechanism, while the transgranular cracking observed in these same alloys is attributed to an oxide stress mechanism. In this section these mechanisms and the conditions under which they occur will be discussed.

Hydride Formation

It has been shown that H_2 can affect both the ductility and the crack propagation behavior of uranium and numerous uranium alloys. The H_2 can be present in the metal at the beginning of a test, introduced into the metal from H_2 gas during a test or introduced as a by-product of the oxidation of uranium by H_2O. The embrittlement of uranium by internal H has been attributed to hydrogen in solution[14] and to the formation of UH_3.[10] The kinetics of embrittlement point toward hydride formation. Beevers and Newman[10] found that the embrittlement increased at increasing strain rates and that the degree of embrittlement was the same at 20°C as at −78°C. These observations are certainly difficult to correlate with a solution mechanism dealing with stress-enhanced diffusion. Similar types of observations have

been made for the embrittlement of α–Ti and α–Zr alloys where the formation of hydride is responsible for the loss of ductility.[9]

Hydride can also form in pure H_2 gas if the protective nature of the oxide found on the alloys is destroyed (oxygen in the gas will also prevent hydride formation and cracking). With precracked specimens the plastic deformation at the crack tip ruptures the oxide, and all uranium alloys that have been tested in H_2 have failed. The failure of the U–0.75% Ti in H_2 has been linked to the formation of UH_3.[24]

Uranium and its alloys react with water to form UO_2 and release H_2, which can then react with the metal to form UH_3. Vaughn and Phalen[52] have proposed that this type of corrosion-induced embrittlement mechanism is responsible for the cracking observed in U–7.5% Nb–2.5% Zr. Burkhart and Lustman[67] have proposed that the disintegration of U–Mo and U–Nb alloys in 343°C water is related to the formation of a metastable hydride phase. Jackson[21] observed hydridelike plates at the surface of U–0.75% Ti specimens tested in humid environments which were not observed in specimens tested in dry environments and proposed that the formation of a hydride was responsible for the embrittlement. The formation of hydride from the reaction with H_2O is more likely to occur in alloys that have very high uranium compositions, because as the uranium concentration increases the reactivity of the alloy increases and the H_2 available for hydriding increases dramatically, see Fig. 32.

The hydride which forms under any of the conditions discussed is a very brittle, incoherent phase which can be ruptured easily to form initiation sites and propagation pathways. Even more importantly, the density of the hydride is low compared to the base metal, 11 g/cm^3 for UH_3 compared to 19.1 g/cm^3 for U. Therefore, its formation in a metal will lead to high stresses. This is illustrated by the crack propagation studies on U–0.75% Ti in H_2. The hydride forms at the crack tip and generates stresses of sufficient magnitude to cause crack propagation even after the applied stress has been removed.[24] The hydrides are also very reactive and easily oxidized by O_2 and H_2O. The oxidation of a hydride phase was proposed to be responsible for the disintegration of uranium alloy oxidation coupons at 343°C in water vapor.[67]

In summary, the reduction of ductility observed in uranium and uranium alloy specimens with internal hydrogen and also in specimens tested in H_2O containing environments is attributed to the formation of UH_3. Stress corrosion crack propagation in lean alloys such as U–0.75% Ti in moist air and in all alloys in H_2 is also attributed by hydride formation. It is proposed that the hydride degrades the metal principally because of the high lattice

strains and internal stresses caused by its low density. Secondary influences include the brittle nature and the reactivity of the hydride.

Anodic Dissolution

The intergranular stress corrosion cracking observed in the more heavily alloyed uranium alloys has been attributed to an anodic dissolution type of mechanism. Zehr[68] has proposed a fairly detailed anodic dissolution mechanism for U–7.5% Nb–2.5% Zr which should be equally applicable to intergranular cracking in other uranium alloys. He proposed that an incubation period is required for the establishment of a differential aeration cell. The oxygen-depleted region is anodic and hence cracking should and does start in the center of a water drop. Waber[69] has observed that current flows between uranium specimens in solutions with different O_2 concentrations. Initiation occurs when the oxide is destroyed by a combination of stress, Cl^-, and low pH. The destruction of passivity in U–7.5% Nb–2.5% Zr by Cl^- has been verified.[51,56] The low pH results from the preferential dissolution of U and Zr which leaves an easily ruptured Nb oxide sponge. Auger analysis showed that the stress corrosion cracking surface is rich in Nb, which gives support to the proposed mechanism.

The work of Stephenson,[51] Bullock and Condon,[56] and Koger[57] supports an anodic dissolution mechanism. All three investigations report that anodic potentials enhance cracking and cathodic potentials either slow or stop cracking. Under cathodic potential control when cracking occurs it was transgranular rather than intergranular.

There are some differences of opinion as to the role of pitting in the stress corrosion cracking process. Koger[50] observed that: (1) pitting in U–7.5% Nb–2.5% Zr occurred in short times in unstressed specimens in the same environments that led to short-time stress corrosion failures in stressed specimens, and (2) pitting always preceded stress corrosion cracking in his tests. He proposed that the electrochemical processes leading to pitting and stress corrosion cracking were the same. Bullock and Condon[56] found that some environments which cause stress corrosion cracking in short times will not lead to pitting in long times, which indicates that pitting is not required for stress corrosion cracking. Tests conducted on U–7.5% Nb–2.5% Zr and U–4.5% Nb in 500-ppm Cl^- solutions showed that stress corrosion cracking will occur in long times at the base of deep pits in unstressed specimens.[46] This was attributed to corrosion product wedging by the insoluble, low-density oxides ($\rho_{UO_2} \simeq 11$ g/cm^3, $\rho_{alloy} \simeq 18$ g/cm^3) formed in the deep pits,

see Fig. 40. The data indicate that while pitting is not a necessary condition for stress corrosion cracking, it is a sufficient condition in stressed uranium alloy specimens and in some cases is sufficient in the absence of stress.

In summary, the intergranular cracking which occurs in the more solute-rich uranium alloys is caused by an anodic dissolution process. Crack initiation occurs when the passivity of the alloys is destroyed by Cl^- and a differential aeration cell. Propagation occurs by the rupture of an oxide sponge depleted in the more active metals in the alloy. H_2 embrittlement is not considered to be a viable mechanism for the intergranular cracking.

Oxide Stress Generation

The transgranular stress corrosion cracking observed in uranium alloy in environments containing O_2 is attributed to an oxide stress mechanism. This type of cracking has been observed in U–Mo, U–Nb, and U–Nb–Zr alloys. Oxidation in uranium and uranium alloys occurs by the diffusion of anions into the metal and not by the diffusion of the large highly charged uranium cation.[70,71] The volume expansion which occurs when UO_2 is formed is approximately 70% and therefore, if the oxide remains coherent, large tensile stresses will be generated in the metal and large compressive stresses will be generated in the oxide.

Cathcart[62] has observed large tensile stresses generated by coherent oxides at higher temperatures on uranium alloys. The oxides formed epitaxially on γ-phase materials and led to increases in the length of oxidation

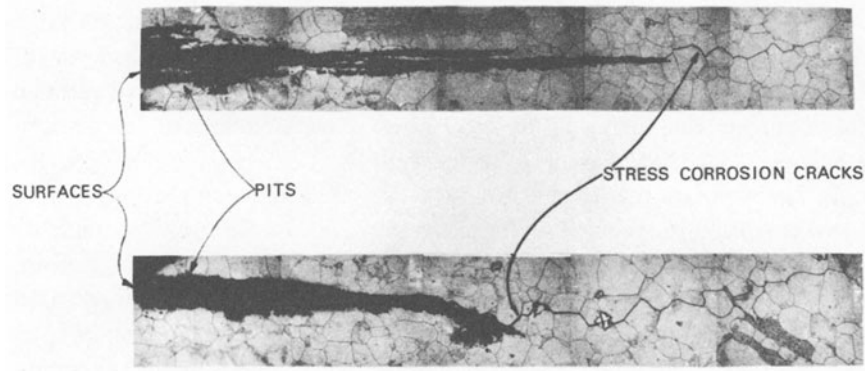

Fig. 40. Pits with stress corrosion cracks in U–4.2% Nb exposed to 40-ppm Cl^- under anodic potential control.

specimens ranging from 0% for U to 125% for U–7.5% Nb–2.5% Zr at 800°C (75 μ of oxide). Cathcart states that all of the alloys formed by the γ stabilizers show evidence of stress generation during oxidation. There is no evidence of stress generation in the equilibrium $\alpha + \gamma$ alloys.[72]

Chirigos[73] proposed that the epitaxial stress caused by the oxide was responsible for the disintegration of U–10% Nb coupons containing 0.25–10% Zr tested in high-temperature water (360°C) and O_2 (300°C). He also exposed specimens to S vapor at 360°C. Failure occurred and was attributed to the formation of an epitaxial U_4S_3 phase.

A similar mechanism has been proposed for the stress corrosion cracking of U–4.5% Nb at room temperature.[45] Several correlations can be made between the stress corrosion cracking and oxidation, supporting an oxide stress mechanism. Cracking in region II, where most of the data were obtained, was dependent on P_{H_2O} in a complex manner. In 125 Torr of O_2, as the relative humidity increases the crack velocity increases, plateaus, and then decreases at very high relative humidities. The oxidation of uranium shows a similar behavior; the rate of formation of UO_2 in O_2 environments increases when water is first added and is independent of R.H. from 5 to 90%.[19] Under saturated conditions a noncoherent hydrated oxide is formed.[19,20] The crack velocity in region II is proportional to K^4. This type of behavior would also be expected for an oxide stress mechanism, i.e., less oxide-generated stress would be necessary for fracture as K increased. Helium ion backscattering experiments have shown that the oxide thickness on the stress corrosion fracture surface decreases as K increases.[74] The experiments also showed thicker oxides are formed on stress corrosion cracking surfaces than on overload surfaces.

In summary, an oxide stress mechanism has been proposed for the transgranular stress corrosion cracking observed in uranium alloys tested in O_2 environments. An epitaxial stress is generated by UO_2 on the alloys which supplements the applied stress and leads to specimen failure.

PROTECTIVE COATINGS

The use of uranium and uranium alloys requires some control of the environment. It has been shown that cracking can occur in 500-ppm Cl^- solutions and in H_2 without any applied load due to corrosion product wedging and residual stresses in the metastable alloys. In dilute Cl^- solutions the threshold for many of the alloys is sufficiently low to preclude their use. The most commonly used form of environmental control for uranium and

uranium alloys has been protective coatings. This section will review the work that has been done on protecting uranium and uranium alloys by coatings.

Oxides

Protective oxides have been formed on uranium by controlling the O_2 supply to the metal[75] and by using controlled anodic potentials.[76,77] The coatings are protective in O_2 and H_2O environments for long times at room temperature, but deteriorate at elevated temperatures. Anodically formed oxides on U–0.75% Ti and U–7.5% Nb–2.5% Zr do not reduce the corrosion rate in O_2 and H_2O environments, but are very abrasion resistant.[77] Studies on the effect of oxides on stress corrosion cracking have shown that at best they are neutral[34] and that they may degrade the performance of the material.[51,59] Therefore, "protective" oxides have not been used on uranium alloys to reduce the stress corrosion cracking susceptibility.

Organic

Orman and Walker[78] evaluated a large number of organic coatings on uranium substrates. They found the best of the coatings were innocuous, while the majority of the coatings were actually corrosive to the uranium. Even the addition of inhibiting pigments such as zinc chromate did not significantly enhance the protection of styrene-butadiene films. In addition to the corrosion caused by constituents in the coating, problems were encountered because of the much lower permeability rate of O_2 compared to H_2O in organic films. With many of the coatings, the O_2 level at the film–metal interface is reduced below that required for inhibition while the H_2O level is high enough to cause corrosion. Leafing aluminum powders were added to two of the innocuous coatings to reduce the diffusion of water through the film. The powders reduce the H_2O permeability by greater than an order of magnitude and significantly reduce the corrosion rate.

Macki and Kochen[79] evaluated the protection afforded to U–4.5% Nb by an epoxy primer and urethane cover coat paint system. They found the coating protected the alloy from general corrosion in a salt fog environment and from stress corrosion cracking in an aqueous chloride (50-ppm Cl^-) environment as long as the paint was not flawed. If the coating was scratched, stress corrosion cracking occurred. Because of the lack of stress corrosion protection that results if the paint contains flaws this type of coating scheme is not considered satifactory for protecting uranium alloys.

Metallic

Metallic coatings have been successfully used to protect uranium and uranium alloys. Electroplated nickel is the most extensively used protective film for uranium. One of the concerns with electroplated coatings is the introduction of hydrogen into the uranium substrate. The sulfamate nickel plating process used extensively in this country does not introduce hydrogen into the bulk of the metal.[22] The total hydrogen content increases, but this is due to an increase on the surface where the H_2 will not adversely affect the mechanical properties of the substrate.[22,80] Less than 0.1 mm of nickel will protect uranium in moist N_2 environments. The result of tests using several thicknesses of Ni are shown in Table 15.

The protection offered to U–0.75% Ti by Ni plate has also been evaluated.[22,26,81] The plating did not improve the ductility of specimens tested in humid environments,[22] presumably because of the fracture of the plating during the test. However, Weirick and Douglas[82] found that 0.012 mm of Ni protects the alloy from corrosion in 25°C salt solutions, while merely 0.005 mm is protective in moist air at 105°C. Nickel coatings are electropositive to U–0.75% Ti and will accelerate stress corrosion cracking once they are flawed.[81] Peterson and Vandervoort[32] found that Ni coatings can also accelerate the stress corrosion cracking of U–10% Mo. While Cd and Zn are electronegative to U–Ti and are protective even if flawed, they will not adhere to the alloy substrate. This led to a duplex coating scheme of Ni plating covered by Zn and followed by a chromate finish, which has successfully protected the alloy from corrosion and stress corrosion.[81]

Ion plated aluminum coatings protect uranium in moist air at temperatures up to 100°C.[83,84] However, the coatings deteriorate with time, and the

Table 15. Corrosion of Nickel-Plated Uranium in Moist Nitrogen[a]

Thickness of plating, mm	Length of test	Hydrogen evolved, ppm
No plating	6 weeks	180 000
0.013	8 days	7 000
0.013	6 weeks	35 000
0.025	6 weeks	15
0.051	6 weeks	10
0.076	7 weeks	0
0.076	30 weeks	0

[a] After Johnson *et al.*, Ref. 22.

corrosion rates will eventually increase.[84] Ion plated aluminum protects U–0.75% wt% Ti from moist air at 100°C for more than 30 days but in 25°C, 50-ppm Cl^- solutions the coatings break down and the corrosion rate after 24 days exposure is greater than that for bare uranium.[81] Flaws in the coating accelerate the stress corrosion cracking because the coating is electropositive to the U–Ti substrate.[81]

Aluminum coatings cathodically protect U–4.5 wt% Nb from stress corrosion cracking.[85,86] McLaughlin and Panousis[85] studied the effect of plasma sprayed, electrodeposited, chemical vapor deposited, and physical vapor deposited aluminum and electroplated cadmium on the stress corrosion cracking behavior of U–4.5% Nb. All of the coatings except for the electrodeposited aluminum, effectively inhibited stress corrosion cracking. Specimens with a gap in the coating to simulate damage were also evaluated, and specimens with 4-mm gaps still effectively protect the uranium alloy. Because the aluminum is consumed in the environment, the coatings break down with time.

The data in the literature show that nickel can be effectively used to protect uranium, but that the effective protection of alloys from stress corrosion cracking requires coatings which are electronegative to the uranium alloy. Aluminum has been used effectively for alloys containing higher alloy addition levels, while the "lean" alloys require zinc or cadmium if galvanic protection is to be achieved.

SUMMARY

Three types of cracking behavior have been observed in uranium alloys. The determination of what type of behavior will be observed is related in part to the reactivity of the specimen, and hence to the amount of alloy addition and not on what alloy addition has been made, and in part to the test environment. The lean alloys and uranium are embrittled by internal H_2 and by H_2O in the environment. This behavior is attributed to the formation of the brittle low-density hydride, UH_3. The intergranular cracking in the solute-rich alloys is attributed to an anodic dissolution mechanism. O_2 and Cl^- destroy passivity in the alloy, and the dissolution of the more active metal constituents leaves an oxidized sponge which is easily ruptured by the applied stress. The transgranular cracking in the solute-rich alloys is attributed to an oxide stress mechanism. The formation of an epitaxial UO_{2+x} oxide on the metal, stresses the metal in tension, and this stress, when combined with the applied stress, results in the fracture of the metal at the crack tip.

Uranium and all of the uranium alloys tested to date are susceptible to embrittlement and/or stress corrosion cracking in environments as innocuous as laboratory air. There are a few options with regard to alloy composition and heat treatment that can be used to minimize the embrittlement and cracking problems in uranium alloys. It has been shown that heat treating metastable uranium alloys to form the equilibrium $\alpha + \gamma$ structure will increase the resistance to stress corrosion cracking. The mechanical properties of the resultant alloys are often as good if not better than the quenched alloys. However, two problems can occur. First, the α phase is not very corrosion resistant even when saturated with an alloy addition, and second, the anisotropic nature of the α phase may lead to dimensional stability problems.

It has been shown that the lean alloys will crack in H_2O while O_2 inhibits cracking and the alloys with higher solute levels will not crack in H_2O but will in O_2. The higher solute alloys are also quite sensitive to Cl^- in aqueous solutions while the lean alloys are to a lesser degree. This type of behavior immediately points out the importance of proper alloy selection if the environment is well-defined and controlled. Protective coatings are used on uranium and uranium alloys in environments where the hostile constituents cannot be removed. Metallic coatings including Ni, Al, and Zn are the most successful.

ACKNOWLEDGMENTS

The author would like to thank K. H. Eckelmeyer and L. J. Weirick for reviewing this manuscript.

REFERENCES

1. W. O. Wilkinson, *Uranium Metallurgy*, Vol. II, *Uranium Corrosion and Alloys*, Interscience, New York (1966).
2. H. L. Yakel, Crystal Structures of Transition Phases Formed in U-16.60 a/o Nb-5.64 a/o Zr Alloys, *J. Nucl. Mater.* **33**, 286–295 (1969).
3. K. Tangri and G. I. Williams, Metastable Phases in the Uranium–Molybdenum System and Their Origin, *J. Nucl. Mater.* **4**, 226–233 (1961).
4. M. Anagnostidis, M. Colombie, and H. Monti, Phases Metastables dans les Alliages Uranium-Niobium, *J. Nucl. Mater.* **11**, 67–76 (1964).
5. R. F. Hills, B. R. Butcher, and B. W. Howlett, The Effect of Cooling Rate on the Decomposition of the γ-Phase in Uranium–Zirconium Alloys, *J. Nucl. Mater.* **16**, 25–38 (1965).

6. R. Bashiwitz, M. Colombie, and M. Foure, Annealing of Metastable Orthorhombic Phases of Uranium–Titanium Containing 4.5 and 9.5% Titanium, *J. Nucl. Mater.* **28**, 246–256 (1968).
7. K. H. Eckelmeyer, in *Physical Metallurgy of Uranium Alloys* (J. J. Burke, D. A. Colling, A. E. Gorum, and J. Greenspan, eds.), Brook Hill, Chestnut Hill, Mass. (1975).
8. G. L. Powell and J. B. Condon, in *Physical Metallurgy of Uranium Alloys* (J. J. Burke, D. A. Colling, A. E. Gorum, and J. Greenspan, eds.), Brook Hill, Chestnut Hill, Mass. (1975).
9. P. Cotterill, The Hydrogen Embrittlement of Metals, *Progr. Mater. Sci.* **9**, 201–301 (1961).
10. C. J. Beevers and G. T. Newman, Hydrogen Embrittlement in Uranium, *J. Nucl. Mater.* **23**, 10–18 (1967).
11. H. Inouye and A. C. Schaffhauser, Low-Temperature Ductility and Hydrogen Embrittlement of Uranium–A Literature Review. Oak Ridge National Laboratory Report ORNL-TM-2563 (July 1969).
12. P. Adamson, S. Orman, and G. Picton, The Effects of Hydrogen on the Tensile Properties of Uranium When Tested in Different Environments, *J. Nucl. Mater.* **33**, 215–224 (1969).
13. G. S. Hanks, J. M. Taub, D. T. Doll, T. J. Jones, and V. Vigil, The Effect of Annealing Media on the Mechanical Properties of Uranium, Los Alamos Scientific Laboratory Report 1619 (Aug. 1963).
14. W. D. Davis, Solubility, Determination, Diffusion and Mechanical Effects of Hydrogen in Uranium, Knolls Atomic Power Laboratory Report KAPL-1548 (Aug. 1956).
15. R. Smith, Atomic Energy Research Establishment Report AWRE-M/R-2700 (1959).
16. G. A. Whitlow and R. Willows, The Effect of Humidity on the Ductility of Uranium, Atomic Weapons Research Establishment Report AWRE O-46/66 (1966).
17. A. N. Hughes, S. Orman, and G. Picton, Environmental Factors Affecting the Mechanical Properties of Uranium. 1. The Effect of Water Vapor, *J. Nucl. Mater.* **33**, 159–164 (1969).
18. A. N. Hughes, S. Orman, G. Picton, and M. A. Thorne, Environmental Factors Affecting the Mechanical Properties of Uranium. 2. The Mechanisms of Water Embrittlement of Uranium, *J. Nucl. Mater.* **33**, 165–172 (1969).
19. S. Orman, in *Physical Metallurgy of Uranium Alloys* (J. J. Burke, D. A. Colling, A. E. Gorum, and J. Greenspan, eds.), Brook Hill, Chestnut Hill, Mass. (1975).
20. N. J. Magnani, The Reaction of Uranium and Its Alloys with Water Vapor at Low Temperatures, Sandia Laboratories Report SAND-74-0145 (Aug. 1974).
21. R. J. Jackson, Effect of Humidity on Tensile Ductility of Uranium-Titanium Alloys, Dow Chemical, Rocky Flats Division Report RFP-2048 (1972).
22. H. R. Johnson, J. W. Dini, and S. W. Zehr, in *Hydrogen in Metals* (L. M. Bernstein and A. W. Thompson, eds.), ASM Materials/Metalworking Technology Series Vol. 2, pp. 325–343, American Society of Metals (1974).
23. N. J. Magnani, The Effects of Environment, Orientation, and Strength Level on the Stress Corrosion Behavior of U–0.75 wt% Ti, *J. Nucl. Mater.* **54**, 108–116 (1974).
24. N. J. Magnani, The Wedging Action of UH_3 During Slow Crack Growth in U–0.75 wt% Ti, *Corrosion* **31**, 337–338 (1975).
25. N. J. Magnani, The Effects of the Environment on the Cracking Behavior of Selected Uranium Alloys, NACE Corrosion 72, Mar., 1972, St. Louis, Mo., Paper 58; Sandia Laboratories Report SCR-72-2661 (Mar. 1972).
26. B. D. McLaughlin and L. L. Stephenson, Private communication, Sandia Laboratories, Albuquerque, N.M. (1973).
27. W. F. Czyrklis and M. Levy, Stress Corrosion Cracking Behavior of Uranium Alloys, *Corrosion* **30**, 181–197 (1974).
28. M. Levy, Private communication, Army Materials and Mechanics Research Center, Watertown, Mass. (Dec. 1973).

29. N. J. Magnani, The Stress Corrosion Cracking Behavior of Two Uranium Alloy Armor Penetrator Materials, Sandia Laboratories Report SLA-74-0304 (Aug. 1974).
30. M. W. Burkart, I. Cohen, and R. K. McGeary in *Advances in Nuclear Engineering*, Vol. 2, p. 197–208, Pergamon, New York (1958).
31. J. W. Pridgeon, Stress Corrosion Cracking in Uranium-Molybdenum Alloys, Union Carbide Y-12 Plant Report Y-1417 (May 1963).
32. C. A. W. Peterson and R. R. Vandervoort, Stress-Cracking in the Uranium 10 w/o Molybdenum Alloy, Lawrence Radiation Laboratory Report UCRL-7769 (May 1964).
33. S. A. Hoenig and H. Sulsona, A Field Emission Microscope Investigation of the Effects of Ambient Atmospheres on the Stress-Corrosion Cracking of Uranium–Molybdenum Alloys, U.S. Government Research and Development Report 68(14), 79 (1968).
34. S. Orman and G. Picton, The Stress-Corrosion Cracking of Uranium–Molybdenum Alloys, Atomic Weapons Research Establishment Report 015/70 (1970).
35. A. M. Nomine, D. Bedere, and D. Miannay, in *Physical Metallurgy of Uranium Alloys* (J. J. Burke, D. A. Colling, A. E. Gorum, and J. Greenspan, eds.), Brook Hill, Chestnut Hill, Mass. (1975).
36. A. M. Nomine, D. Bedere, R. Robin, and D. Miannay, Mechanical Study of the Stress Corrosion of a U-10 Mo Alloy, in Colloque sur la Rupture de Materiaux, Grenoble (Jan. 1972), Sandia Laboratories Translation SC-T-722510 (May 1972).
37. C. A. W. Peterson, A Stress-Cracking Study of a Gamma Extruded U–8 w/o Mo–0.50 w/o Ti Alloy, Lawrence Radiation Laboratory Report UCRL-14132 (Apr. 1965).
38. A. M. Nomine, D. Bedere, and D. Miannay, Mechanical Quantities Associated with Stress Corrosion of the U–10 Mo Alloy, in Colloque sur la Rupture de Materiaux, Grenoble (Jan. 1972), Sandia Laboratories Translation SC-T-722508 (May 1972).
39. R. Willows and G. A. Whitlow, High Strength Uranium Alloys: Mechanical Properties, Atomic Weapons Research Establishment Report AWRE 0-34/70 (May 1970).
40. G. A. Whitlow, Stress Corrosion of Uranium Alloys, Atomic Weapons Research Establishment Report AWRE 0-49/66 (July 1966).
41. S. W. Zehr, in *Physical Metallurgy of Uranium Alloys* (J. J. Burke, D. A. Colling, A. E. Gorum, and J. Greenspan, eds.) Brook Hill, Chestnut Hill, Mass. (1975).
42. N. J. Magnani and H. Romero, The Reaction of Water Vapor with U–7½ wt% Nb–2½ wt% Zr and U–4½ wt% Nb, Sandia Laboratories Report SC-RR-720635 (Sept. 1972).
43. N. J. Magnani, Stress Corrosion Cracking in Quenched and in Underaged U–6 wt% Nb, Sandia Laboratories Report SAND-75-0191 (June 1975).
44. J. M. Macki and R. L. Kochen, The Stress-Corrosion Cracking Behavior of the U–4.2 wt% Nb Alloy Aged 80 Hours at 260°C, Dow Chemical, Rocky Flats Division Report RFP-1824 (Mar. 1972).
45. N. J. Magnani, to be published.
46. N. J. Magnani, The Effect of Chloride Ions on the Cracking Behavior of U–7.5 wt% Nb–2.5 wt% Zr and U–4.5 wt% Nb, *J. Nucl. Mater.* **42**, 271–277 (1972).
47. J. M. Macki and R. L. Kochen, The Stree-Corrosion Cracking of Underaged and Overaged U–2.3 wt% Nb in an Aqueous Chloride Environment, Dow Chemical, Rocky Flats Division Report RFP-1904 (August 1972).
48. A. R. Miller, The Stress Corrosion Cracking of U–Nb alloys in air, submitted to *Corrosion*.
49. J. W. Koger, Stress-Corrosion Cracking of Uranium Alloys, Union Carbide Y-12 Plant Report Y-DA-5624 (Dec. 1973).
50. B. D. McLaughlin, L. L. Stephenson, and C. J. Miglionico, Influence of aging time and temperature on the susceptibility of γ-quenched U–5 wt% Nb alloy to stress corrosion cracking, *Corrosion* **28**, 35–38 (1972).
51. L. L. Stephenson, A Survey of Factors Which Influence Stress Corrosion Crack Initiation in Several Uranium Base Alloys, Sandia Laboratories Report SC-DR-70-718 (Oct. 1970).

52. D. A. Vaughn and D. I. Phalen, Summary Report on Mechanisms of Failure in Mulberry Alloy (U–7.5% Nb–2.5% Zr), Battelle Memorial Institute (Oct. 1969).
53. L. J. Weirick and C. W. Schoenfelder, The Effect of Oxygen, Chloride Ions and Water Vapor on Crack Initiation in U–7½ wt% Nb–2½ wt% Zr, *Corrosion* **30**, 169–174 (1974).
54. N. J. Magnani, H. Romero, and C. J. Miglionico, A Study of the Stress Corrosion Cracking Behavior of Mulberry (U–7.5% Nb–2.5% Zr), Sandia Laboratories Report SC-RR-70-371 (May 1970).
55. A. R. Miller, Effect of Relative Humidity on the Stress Corrosion Cracking of U–7.5% Nb–2.5% Zr alloy, *Corrosion* **30**, 177–178 (1974).
56. J. S. Bullock IV and J. B. Condon, Electrochemical and Other Studies of a Uranium Alloy Exhibiting Stress-Corrosion Cracking, Union Carbide Y-12 Plant Report Y-1821 (Feb. 1972).
57. J. W. Koger, Variables Which Influence the Stress-Corrosion Cracking of Uranium–7.5 Niobium–2.5 Zirconium Alloy, Union Carbide Y-12 Plant Report Y-1965 (Jan. 1975).
58. L. J. Weirick, The Effect of Heat Treatment upon the Stress-Corrosion Cracking of Mulberry (U–7.5 Nb–2.5 Zr), *Corrosion* **31**, 5–14 (1975).
59. C. A. W. Peterson and W. J. Steele, Delayed Cracking Study in U–7.5% Nb–2.5% Zr, Lawrence Radiation Laboratory Report UCID-15256 (Dec. 1967).
60. C. Chen, The Stress-Corrosion Cracking Behavior of Uranium–7.5% Nb–2.5% Zr, Master's Thesis, New Mexico Institute of Mining & Technology, Socorro, N. M. (Oct. 1974).
61. C. A. Colmenares, in *Progress in Solid State Chemistry* (J. O. McCaldin and G. Somorjai, eds.), Vol. 9, Pergamon, Elmsford, N.Y. (1974).
62. J. V. Cathcart, in *Physical Metallurgy of Uranium Alloys* (J. J. Burke, D. A. Colling, A. E. Gorum, and J. Greenspan, eds.), Brook Hill, Chestnut Hill, Mass. (1975).
63. N. J. Magnani, Stress Corrosion Cracking of Mulberry, *Corrosion* **10**, 406–408 (1970).
64. M. Levy, C. V. Zabielsky, and G. N. Sklover, Corrosion Behavior of Depleted Uranium–Titanium and Uranium–Molybdenum Alloys, Army Materials and Mechanics Research Center Report AMMRC-TR-73-11 (Mar. 1973).
65. J. Brettle and S. Orman, Stress Corrosion Testing Using a Potentiostatic Dynamic Strain Technique, Atomic Weapons Research Establishment Report AWRE 0 22/73 (Apr. 1973).
66. M. A. Beaubron, Influence de la Teneur en Carbone sur la Corrosion sous Tension d'un Alliage U–Mo a 10% en Poids Mo dans l'air Humide a 20°C, *J. Nucl. Mater.* **43**, 351–353 (1972).
67. M. W. Burkhart and B. Lustman, Corrosion Mechanisms of Uranium-Base Alloys in High Temperature Water, *Trans. AIME* **212**, 26–31 (1958).
68. S. W. Zehr, A Study of the Intergranular Cracking of U–7.5 wt% Nb–2.5 wt% Zr (mulberry) Alloy in Aqueous Chloride Solutions, *Corrosion* **28**, 196–205 (1972).
69. J. T. Waber, A Review of the Corrosion Behavior of Uranium, Los Alamos Scientific Laboratory Report LA-2035 (Apr. 1956).
70. C. I. Evans, Short-Term Oxidation of Uranium in Air in the Range 250–325°C, *J. Inst. Met.* **94**, 187–189 (1966).
71. O. Kubaschewski and B. E. Hopkins, *Oxidation of Metals* Academic Press, New York (1962).
72. J. V. Cathcart, R. E. Pawel, and G. F. Petersen, Oxidation Properties of Two Uranium Alloys (U–16.6 at.% Nb–5.6 at.% Zr and U–21 at.% Nb), *Oxid. Met.* **3**, 497–521 (1971).
73. J. N. Chirigos, in *Physical Metallurgy of Stress Corrosion Fracture* (T. N. Rhodin, ed.), pp. 70–78, Interscience, New York (1959).
74. S. T. Picraux and S. M. Myers, Private communication, Sandia Laboratories, Albuquerque, N. M. (1972).

75. G. S. Petit, R. R. Wright, C. A. Krenberger, and C. W. Weber, Formation of Corrosion-Resistant Oxide Films on Uranium, Union Carbide, Oak Ridge Gaseous Diffusion Plant Report K-1778 (Oct. 1969).
76. O. Flint, J. T. Polling, and A. Charlesby, The anodic oxidation of uranium, *Acta. Met.* **2**, 696–712 (1954).
77. T. S. Prevender, Private communication, Sandia Laboratories, Albuquerque, N. M. (Nov. 1974).
78. S. Orman and P. Walker, The Corrosion of Uranium and its Prevention by Organic Coatings, *J. Oil Colour Chem. Ass.* **48**, 235–255 (1965).
79. J. M. Maeki and R. L. Kochen, The Corrosion and Stress-Corrosion Cracking of Painted U–4.2 wt% Nb, Dow Chemical, Rocky Flats Division Report RFP-1891 (Aug. 1972).
80. J. W. Dini, H. R. Johnson, and C. W. Schoenfelder, Corrosion Behavior, Mechanical Properties, and Long Term Aging of Nickel Plated Uranium, Sandia Laboratories Report SAND-74-8503 (Dec. 1974).
81. L. J. Weirick, Evaluation of Metallic Coatings for the Corrosion Protection of a Uranium–3/4 wt% Ti Alloy, Sandia Laboratories Report SLL-73-5024 (Feb. 1974).
82. L. J. Weirick and D. L. Douglas, The Effect of Thin Electrodeposited Nickel Coatings on the Corrosion Behavior of U–0.75 Ti, Sandia Laboratories Report SLL-74-5010 (June 1974).
83. D. M. Mattox and R. D. Bland, Aluminum Coating of Uranium Reactor Parts for Corrosion Protection, *J. Nucl. Mater.* **21**, 349–352 (1967).
84. R. D. Bland, A Parametric Study of Ion-Plated Aluminum Coatings on Uranium, *Electrochem. Tech.* **6**, 272–278 (1968).
85. B. D. McLaughlin and N. T. Panousis, Protective Metallic Coatings for a γ-Quenched U–5 wt% Nb alloy, *J. Nucl. Mater.* **43**, 343–346 (1972).
86. J. M. Macki, G. Mah, R. L. Kochen, and C. W. Nordin, The Stress-Corrosion Cracking of Aluminum Coated U–4.5 wt% Nb, *J. Nucl. Mater.* **47**, 173–176 (1973).